7

A Combined Petrological-Geochemical Study of the Paleozoic Successions of Iraq

A. I. Al-Juboury
Research Center for Dams and Water Resources, Mosul University, Mosul
Iraq

1. Introduction

Combination of petrographic, mineralogic and geochemical data form the main task of petrologic studies that aim to discuss the provenance history of sedimentary siliciclastic rocks. Provenance analysis serves to reconstruct the pre-depositional history of sediments or sedimentary rocks. This includes the distance and direction of transport, size and setting of the source region, climate and relief in the source area, tectonic setting, and the specific types of source rocks (Pettijohn et al. 1987). Provenance models of sedimentary rocks have, generally taken into account the mineralogical and/or chemical composition of sandstones and shales. Intermingling of detritus from different sources and recycling complicate the determination of sedimentary provenance. Many attempts have been made to refine provenance models using the framework composition and geochemical features (Bhatia and Crook, 1986; Dickinson, 1985; Roser and Korsch, 1988; Zuffa, 1987; Armstrong-Altrin et al., 2004; Umazano et al., 2009 and many others). The chemical composition of the whole rock can provide constraints on provenance because abundance and ratios involving relatively immobile elements are generally not affected by diagenetic processes. Thus chemical data might indicate, in a given sediments, the presence of components which are hard to identify petrographically owing to diagenetic alteration. The geochemical signatures of clastic sediments have been used to find out the provenance characteristics including; the composition of source area (Armstrong-Altrin et al., 2004; Jafarzadeh and Hosseini-Barzi, 2008; Armstrong-Altrin, 2009; Dostal and Keppie, 2009; Umazano et al., 2009; Bakkiaraji etal., 2010), to evaluate weathering processes (Absar et al., 2009; Chakrabarti et al., 2009; Hossain et al., 2010), and to palaeogeographic reconstructions (Ranjan and Banerjee, 2009; Zimmermann and Spalletti, 2009; de Araújo et al., 2010).

The Paleozoic succession of Iraq is exposed in the northernmost part of the country (Fig. 1) and can be traced south and west wards in the subsurface. The Paleozoic succession includes five intracratonic sedimentary cycles, the individual cycles are predominantly siliciclastic, or mixed siliclastic-carbonate units. Sedimentation was mainly controlled by tectonic and eustatic processes which governed the formation of depositional centres, the arrangement of accommodation space within these centres, and the pattern of infilling of the basins (Al-Juboury and Al-Hadidy, 2009). Interbedded sandstones and shales from the Ordovician Khabour Formation and the Devonian-Carboniferous Kaista Formation are selected for this study to evaluate their provenance history.

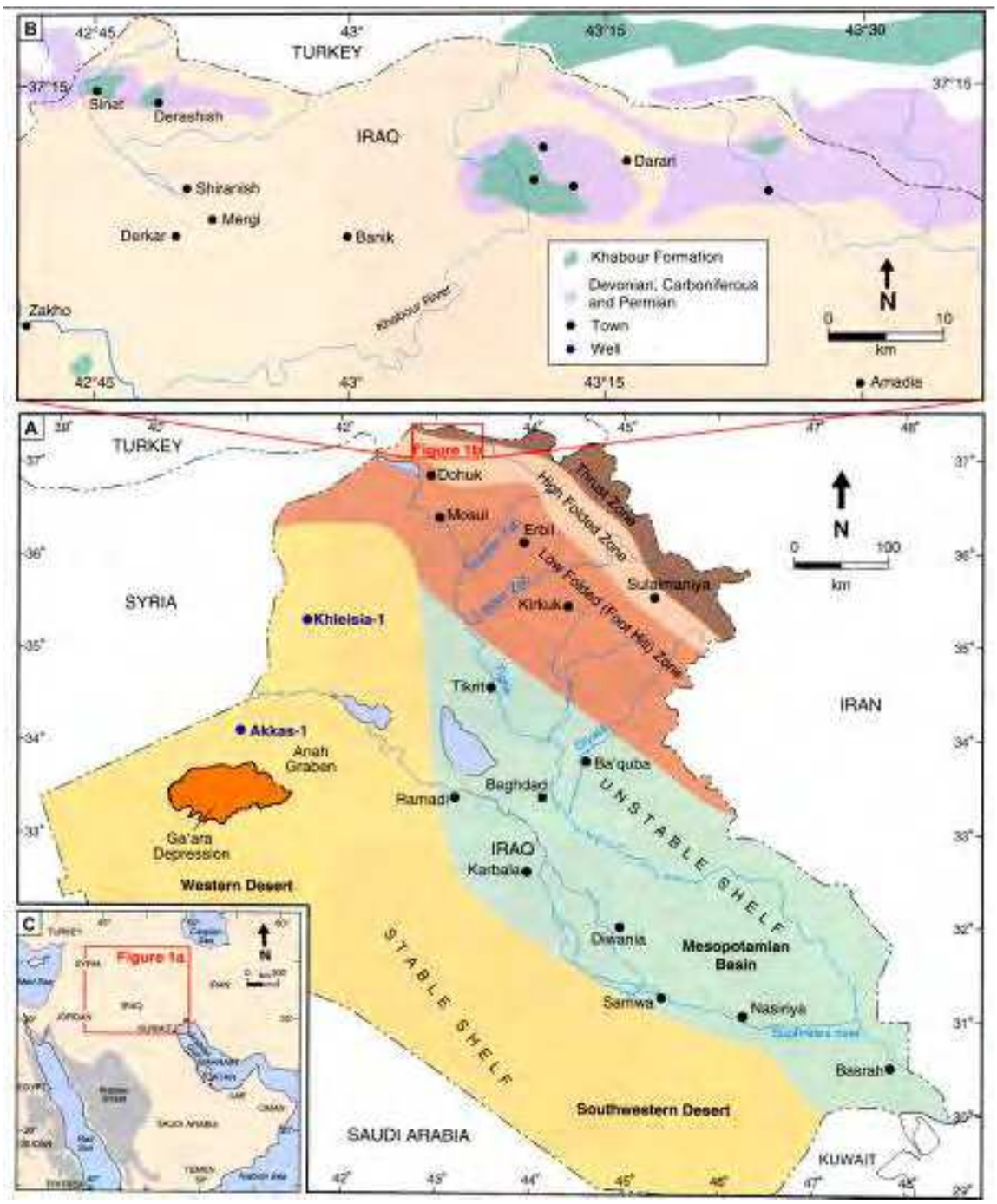

Fig. 1. (a) The structural provinces of Iraq after Buday and Jassim (1987) and the location of the Akkas-1 and Khleisia-1 wells. (b) Paleozoic outcrops in the Ora region including the Khabour and Kaista formations (modified from Al-Omari and Sadiq, 1977). (c) Inset map shows countries neighboring Iraq.

Geochemically derived provenance information from the Paleozoic shales is compared with data from petrographical and geochemical studies of interbedded sandstones and siltstones, in order to assess agreement between the two approaches and to refine knowledge of the provenance for these Paleozoic successions of Iraq.

2. Geologic setting

The stratigraphy of Iraq is strongly affected by the structural position of the country within the main geostructural units of the Middle East region as well as by the structure within Iraq. Iraq lies in the border area between the major Phanerozoic units of the Middle East, i.e., between the Arabian part of the African Platform (Nubio-Arabian) and the Asian branches of the Alpine tectonic belt. The platform part of the Iraqi territory is divided into two basic units, i.e., a stable and an unstable shelf (Figure 1). The stable shelf is characterized by a relatively thin sedimentary cover and the lack of significant folding. The unstable shelf has a thick and folded sedimentary cover and the intensity of the folding increases toward the northeast (Buday 1980). In the Paleozoic, much of the region was covered intermittently by shallow epeiric seas that bordered lowlands made up of portions of the Nubio-Arabian shelf (Al-Sharhan and Nairn 1997). The areal extent of the shelf seas change in response to succeeding transgressions and regressions as the Paleozoic era advanced and their setting varied between tropical and temperate latitudes of the southern hemisphere (Beydoun 1991).

Sedimentary basins of the Paleozoic of Iraq are characterized by the dominance of clastic deposition in the Ordovician and Silurian, with the formation of shallow epeiric seas, which covered large areas of the Arabian Platform. The Arabian Plate represented the northeastern part of the African Plate which extending north and northeastwards over the region now occupied by Iraq, the Arabian Gulf Region, Afghanistan, Pakistan, central, southern, and southeastern Turkey (Numan, 1997). This region represents the northern margin of Gondwana overlooked the southern margins of the Paleo-Tethys Ocean. Epicontinental seas regressed and transgressed over vast areas throughout the Paleozoic, resulting in generally various bed thicknesses and lithotype associations with persistence of facies and absence of unconformities. These characteristics contravene notions (Beydoun, 1991 and Best et al., 1993) that is represented a Gondwana passive margin (Numan, 1997). This region of the Arabian Plate was evolved in AP2 tectonostratigraphic megasequence through intra-cratonic setting (Northern Gondwana land intraplate Paleozoic basin sensu Numan, 1997) with an extension, subsidence and mild uplifting tectonic phase close to Paleo-Tethys passive margin at moderate to high southern latitudes and dominance of clastic sedimentation (Husseini, 1992; McGillivary and Husseini, 1992).

The Paleozoic succession includes five intracratonic sedimentary cycles predominated by siliciclastic, or mixed siliclastic-carbonate units. The Paleozoic cycles commence within the Ordovician with the deposition of the Khabour Formation. This was followed in Silurian times by the Akkas Formation and this is unconformably overlain by the Middle-Late Devonian to Early Carboniferous cycle, represented by the Chalki, Pirispiki, Kaista, Ora and Harur formations. The overlying Permo-Carboniferous cycle is represented by the Ga'ara Formation. The uppermost cycle is late Permian in age and comprises the Chia Zairi Formation. The Paleozoic succession contains a series of muddy units distributed

throughout the stratigraphy. The oldest is found in the lower part of the Ordovician Khabour Formation and comprises up to c. 600 m of black fissile shales. Shale units are also present elsewhere within the Ordovician succession, although here they are generally interbedded with sandstones and siltstones. Calcareous shale alternates with sandstone and few dolomites in the Famenian Kaista Formation.

The black shales near the base of the Khabour Formation in western Iraq were also recognized as a maximum flooding surface within the middle part of the Hiswah Formation in Jordan, near the base of the Swab Formation in Syria, and near the base of Saih Nihayda Formation in Oman (Sharland et al. 2001). It is also recognized by Al-Sharhan and Nairn (1997) as a major regional maximum flooding surface separating the Sauk and Tippecanoe sequences sensu Sloss (1963). Lithofacies analysis of the succession in the well Akkas-1 from the western desert of Iraq (Al-Juboury and Al-Hadidy, 2009) revealed that five lithofacies can be recognized. These are; basinal shale facies, transition (shelf to shore-face) facies, tidal storm regressive and transgressive facies, and the near-shore facies.

In surface section of extreme north Iraq, the Khabour Formation consists of alternations of thin-bedded, fine-grained sandstones, quartzites (Cruziana-rich) and silty micaceous shales, olive-green to brown in color. The quartzites are generally cross-bedded, both finely and coarsely, the thicker beds being generally white in color. Bedding planes are usually well-surfaced with smooth films of greenish micaceous shales. Quartzite beds are occasionally truncated by the overlying beds and show fucoids markings, in filled trails and burrows, pitted surfaces and, other bedding-plane structures of unknown origin. Metamorphism is very slight in the thin-bedded shales with quartzites, and almost unnoticeable in the thicker shale beds, (van Bellen et al., 1959). Karim (2006) has noted that the formation in north Iraq was deposited in a spectrum of environments including fluviatile, deltaic, shelf, slope, and deep marine. The depositional environment of the Kaista Formation is interpreted to be a mixed fluvial-marine system. The lower part of the Kaista Formation represents the continuation of clastic influx from the former regressive sequences of the Pirispiki Formation (early Late Devonian), followed by a transgressive phase characterized by a shale facies with glauconite and thin dolostones (Al-Juboury and Al-Hadidy. 2008).

3. Materials and methods

Sandstones and shale samples were selected from the Paleozoic Khabour and Kaista formations from west and North Iraq (Figs. 2 and 3). Totally 50 samples were collected and 24 sandstone (medium to coarse-grained) samples were studied for modal analysis. Between 300-350 grains were counted in each thin section using the Gazzi-Dickinson method to minimize the dependence of rock composition on grain size. Framework parameters (Ingersoll & Suczek, 1979) and detrital modes of sandstones from the studied formations are given in Table 1.

Whole-rock chemical analyses were performed for 28 samples, which include 16 sandstone and 12 shale. Analyses were performed by X-Ray Fluorescence (XRF) and inductively couple plasma-mass spectrometry (ICP-MS) at laboratories of Earth Science Department of Royal Holloway of London University, UK and the results are provided in Tables 2 and 3 respectively. Some X-Ray diffraction (XRD) and scanning electron microscope (SEM)

analyses were done at laboratories of Wollongong University (Australia) and Bonn University (Germany).

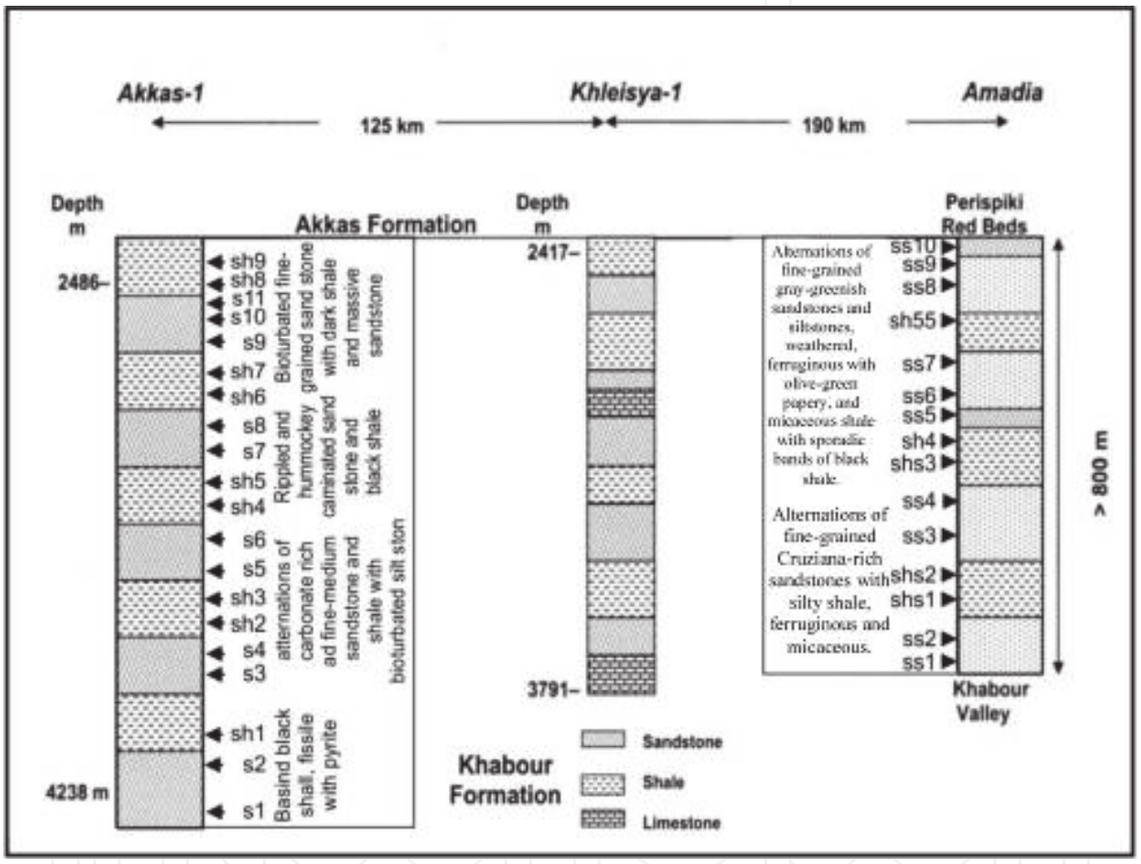

Fig. 2. Generalized lithological succession of the Khabour Formation in Akkas-1 and Khleisya wells of west Iraq and outcrop section at Amadia on north Iraq showing lithological description and location of the analyzed samples.

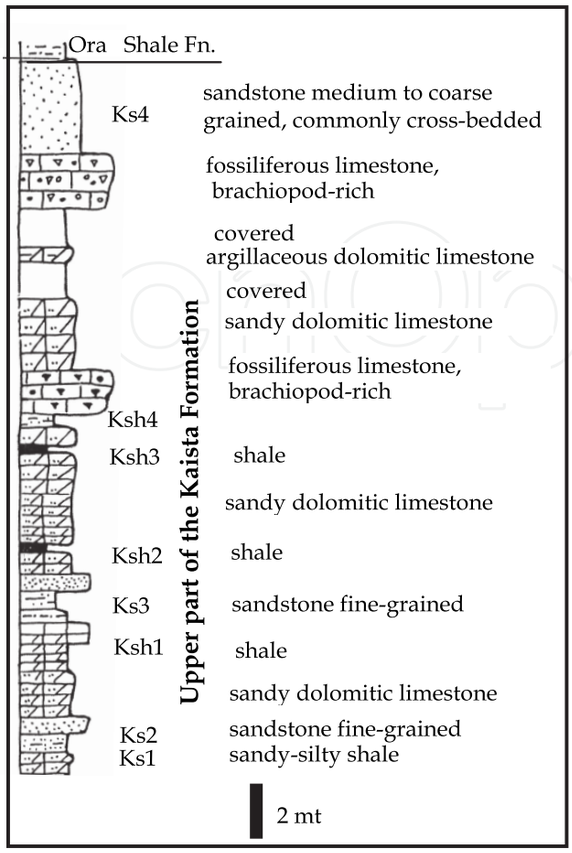

Fig. 3. lithological section of the upper part of the Kaista Formation at Ora region of extreme north Iraq

4. Results

4.1 Sandstone petrography

Quartz is the most dominant constituent of the studied Khabour and Kaista sandstones. Mono-crystalline quartz is the most abundant framework grains. The monocrystalline quartz grains with or without inclusions, the most common inclusions recognized are vacuoles, acicular rutile, spherulitic zircon, muscovite, apatite and iron oxides. Straight to slightly undulatory extinction is frequent type in the quartz studied. According to the genetic and empirical classification of the quartz types (Folk, 1974), the monocrystalline quartz grains are dominantly plutonic and polycrystalline quartz grains are recrystallized and stretched metamorphic types. Sedimentary (Ls), metasedimentary (metamorphic, Lm), and volcanic lithics (Lv), occur in few and varying proportions throughout the sequences of the Khabour and Kaista sandstones (Figs. 4 and 5). Sedimentary lithics (Ls) are the major rock fragments and are dominantly chert. The feldspars are dominated by plagioclase, untwined orthoclase, and twinned microcline (cross-hatching). Mica commonly observed in the studied sandstones in forms of mica laths and biotite. All samples contain accessory minerals, in minor or trace amounts. The dominant heavy minerals identified are zircon, tourmaline, and rutile. Framework composition of the studied Paleozoic sandstones varies from litharenite (sublitharenite, chertarenite) to subarkose and few quartzarenites (Fig. 6). The sandstones are generally cemented by carbonates, secondary silica, ferruginous, and clayey materials.

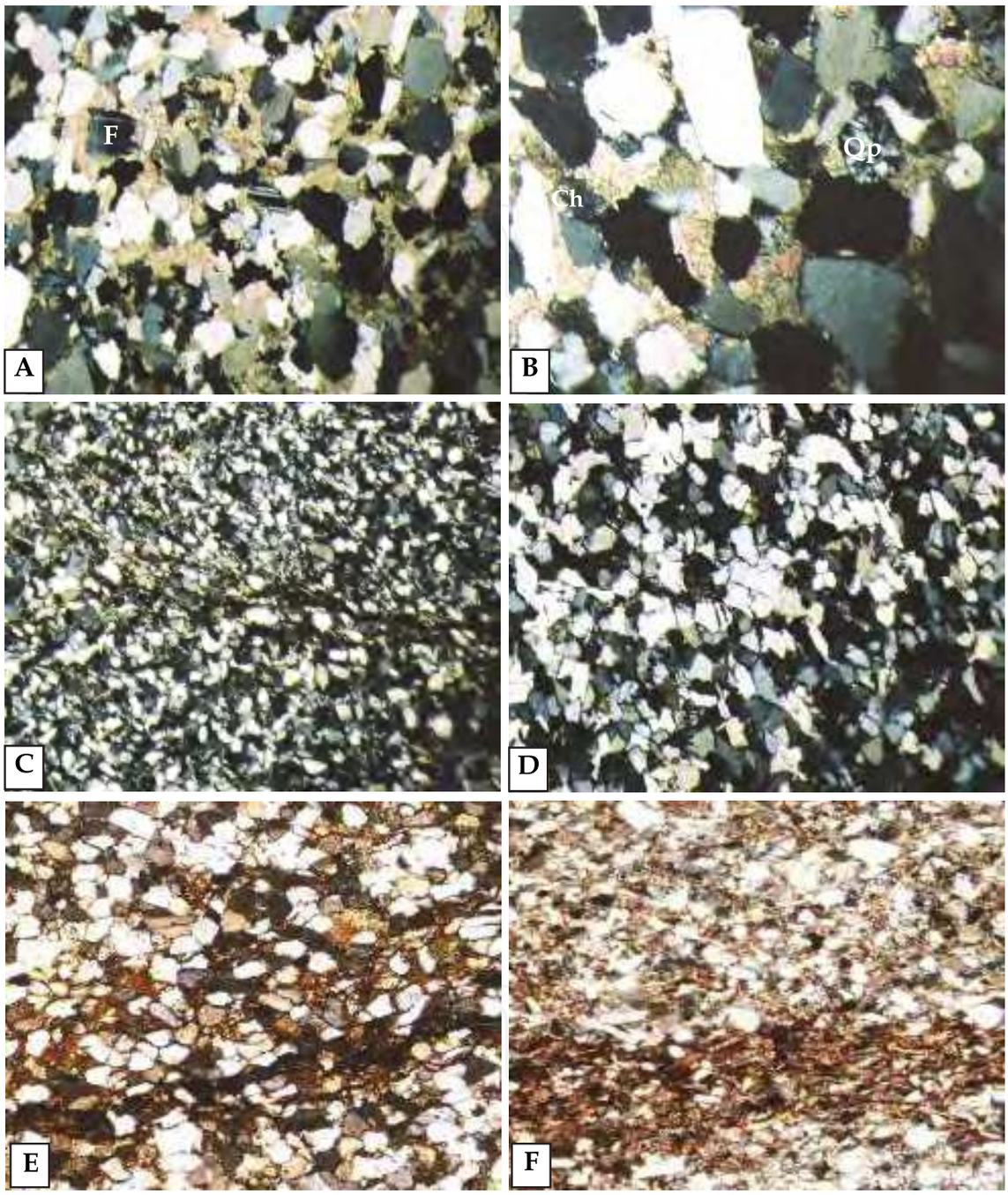

Fig. 4. Photomicrographs of the Khabour sandstones showing (a), monocrystalline quartz and fresh feldspar (F) in carbonate cemented medium grained sandstone. (b), polycrystalline quartz (Qp) and chert (Ch) in medium grained sandstone, note the corroded edges of quartz grains (c), fine-grained sanstones with mica laminations (d), fine-medium grained sandstone, pure quartzarenite with very rare calcite cement patches (e), ferruginous medium grained sandstone (f) fine-grained poorly sorted micaceous sandstone

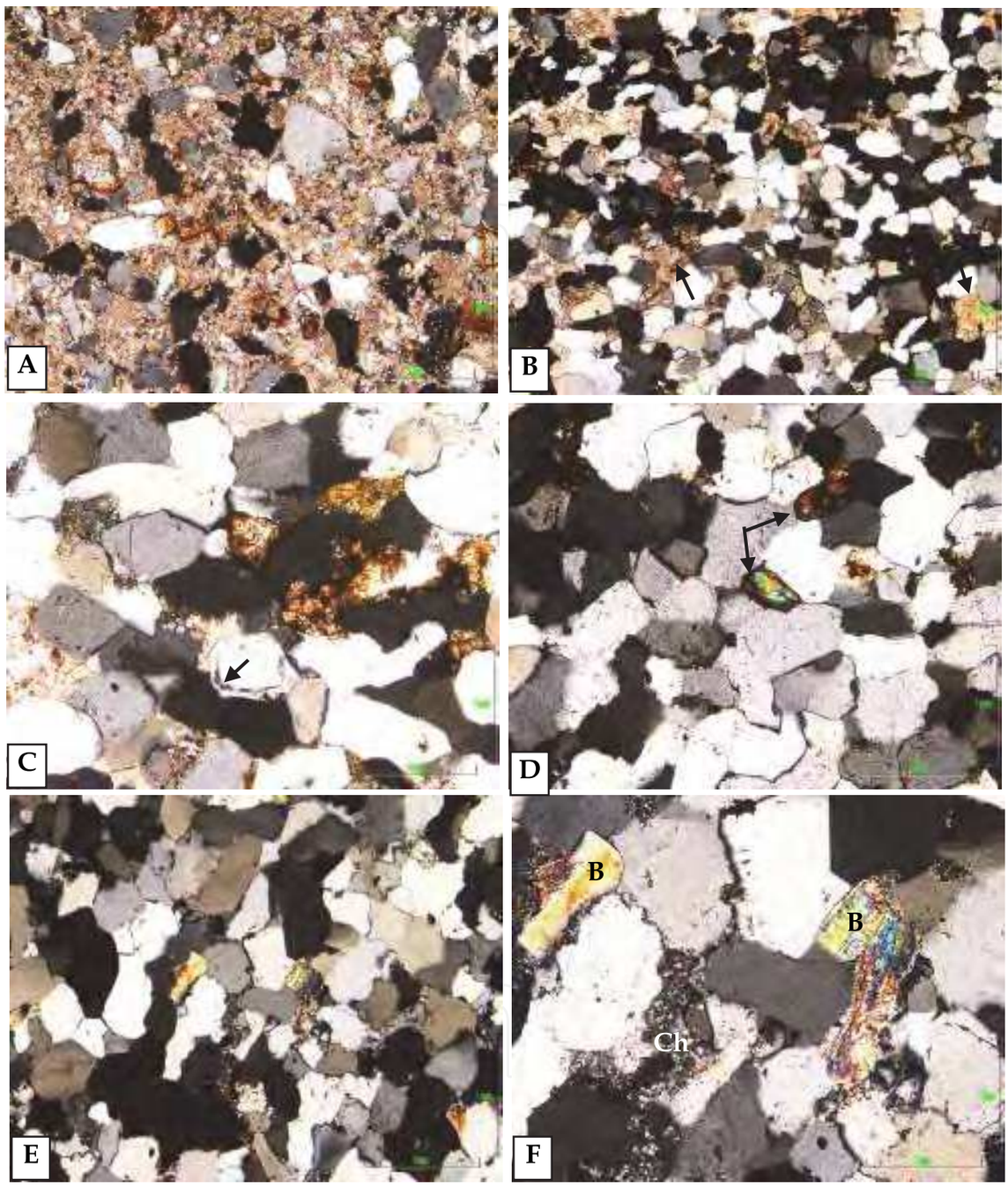

Fig. 5. Photomicrographs of the kaista sandstones showing (A), monocrystalline quartz grains floating in carbonate cement, (B), sandstone with patchy carbonate cement (arrows), (C), iron oxides (sulphides) scattered in quartz rich sandstone, note secondary quartz overgrowth over detrital quartz grain with a chlorite rim between them, (D), highly compacted quartzarenite, note the sutured contacts between grains and two common zircon heavy mineral grains (arrows), (E, and enlarged view in F), compacted sandstone with long-tangential contacts , note chert grains (Ch) and common biotite (B).

Sample	Qm	Qp	Qt	P	K	Ft	Lv	Lm	Ls	Lt (RF)	Qm %	Qp %	Lm %	Lv %	Ls %	Qt %	F %	Lt %	Mtx	Cement C, D, F, S	Others
S1	59	5	64	5	6	11	--	---	4	4	92	8	---	---	100	81	14	5	2	18	1
S2	58	7	65	7	5	12	--	1	2	3	89	11	34	---	66	81	15	4	7	11	2
S3	66	3	69	7	3	10	1	1	2	4	95	5	25	25	50	83	12	5	2	9	6
S4	65	2	67	6	3	8	1	---	3	4	97	3	---	34	66	85	10	5	3	11	7
S5	60	3	63	4	5	9	--	1	1	2	95	5	50	---	50	85	12	3	3	10	13
S6	57	3	60	3	3	6	--	---	1	1	95	5	---	---	100	90	9	1	6	8	19
S7	55	3	58	5	1	6	1	---	2	3	95	5	---	34	66	87	9	4	3	8	22
S8	57	3	60	7	3	10	--	1	3	4	95	5	25	---	75	81	14	5	1	7	18
S9	63	7	70	8	6	14	2	---	2	4	90	10	---	50	50	80	16	4	1	7	4
S10	62	4	66	7	3	10	1	1	1	3	94	6	33	33	34	84	13	3	2	12	7
S11	59	4	63	4	4	8	--	---	2	2	93	7	---	---	100	83	11	6	2	18	7
Ss1	65	6	70	4	3	7	1	2	1	4	93	7	50	25	25	86	9	5	3	11	5
Ss2	62	2	64	4	5	9	---	1	1	2	97	3	50	---	50	85	12	3	2	18	5
Ss3	57	5	62	4	4	8	1	---	6	7	92	8	---	14	86	81	10	9	1	12	10
Ss4	61	3	64	4	6	10	2	1	5	8	95	5	12	25	63	78	12	10	1	11	6
Ss5	58	2	60	4	3	7	3	1	5	9	96	4	11	33	56	79	9	12	2	12	10
Ss6	58	2	60	2	4	6	1	1	5	7	96	4	14	14	72	82	8	10	3	18	6
Ss8	56	2	58	2	5	7	1	1	3	5	97	3	20	20	60	83	10	7	3	18	9
Ss9	57	2	59	4	2	6	1	1	3	5	97	3	20	20	60	84	9	7	4	18	8
Ss10	58	2	60	4	3	7	---	1	5	6	96	4	17	---	83	82	10	8	4	15	8
Ks1	52	1	53	1	1	2	---	----	1	1	98	2	----	---	100	95	3	2	4	32	8
Ks2	59	1	60	1	2	3	---	---	2	2	98	2	----	---	100	92	5	5	7	22	6
Ks3	71	1	72	-	3	3	1	---	5	6	99	1	---	17	83	89	4	7	3	11	5
Ks4	74	2	76	1	2	3	---	---	7	7	97	3	---	---	100	88	4	8	2	9	3

Table 1. Detrital and authigenic modes of 24 selected samples of Khabour and Kaista sandstones. Qm, monocrystalline quartz, Qp, polycrystalline quartz, Qt, total quartz, P, plagioclase, K, K-feldspar, Ft, total feldspar, Lv, igneous rock fragments, Lm, metamorphic rock fragments, Ls, sedimentary (chert) rock fragments, Lt, total (labile) rock fragments, Mtx, matrix, Cements (C, calcite, D, dolomite, F, ferruginous, S, sericite and illite), others mostly iron oxides, sulphides and heavy minerals.

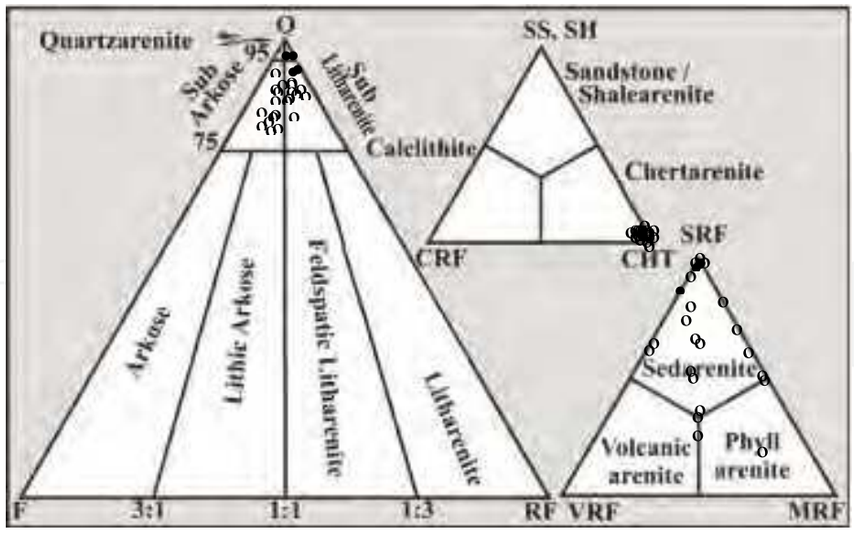

Fig. 6. Minerlaogical classification of the Khabour and Kaista sandstones (Folk, 1974). Q, total quartz; F, Feldspar; RF, rock fragments, SRF, sedimentary rock fragments; VRF, volcanic (igneous rock fragments); MRF, metsedimentary (metamorphic) rock fragments; CHT, chert; CRF, carbonate rock fragments ; SS, sandstone, and SH, shale.
Open circles represents Khabour sandstones and solid circles are Kaista sandstone samples

4.2 Geochemistry

4.2.1 Major elements

Major element distribution reflects the mineralogy of the studied samples. Sandstones are higher in SiO_2 content than shales (Tables 2 and 3 and Fig. 7). Similarly, shales are higher in Al_2O_3, K_2O, Fe_2O_3 and TiO_2 contents than sandstones, which reflect their association in clay-sized phases (Cardenas et al., 1996; Madhavaraju and Lee, 2010). The Al_2O_3 abundances are used as normalization factor to make possible the comparison between different lithologies as it is likely to be immobile during weathering, diagenesis, and metamorphism (Bauluz et al., 2000). In Fig. 7, major oxides are plotted against Al_2O_3. Average UCC(Upper Continental Crust) and PAAS (post Archaean Australian shale) values (Taylor and McLennan, 1985) are also included for comparison. Among other major elements Fe_2O_3, MgO, K_2O, TiO_2 and P_2O_5 are consequently showing strong positive correlations with Al_2O_3, whereas CaO, Na_2O and MnO do not have any trend (Fig. 7). This, strong positive correlations of major oxides with Al_2O_3 indicate that they are associated with micaceous/clay minerals.
The studied samples are normalized to UCC (Taylor and McLennan, 1985) and are given in Fig 8. In comparison with UCC the concentrations of most major elements in sandstones are generally similar, except for Na_2O, with consistently lower average relative concentration value specially for the Kaista sandstones. The depletion of Na_2O (< 1%) in sandstones can be attributed to a relatively smaller amount of Na-rich plagioclase in them, consistent with the petrographic data. K_2O and Na_2O contents and their ratios (K_2O/Na_2O > 1) are also consistent with the petrographic observations, according to which K-feldspar dominates over plagioclase feldspar and common presence of mica as veinlets and patchy distribution in the sandstones of the Khabour Formation (Fig. 4). Some of Kaista sandstones are enriched in CaO and MgO due to the presence of diagenetic calcite and dolomite cements.
In comparison with UCC, the studied shales are low in CaO and Na_2O contents and high in Al_2O_3, K_2O, and TiO_2 contents. Whereas, Kaista shales are enriched in Fe_2O_3 in comparison

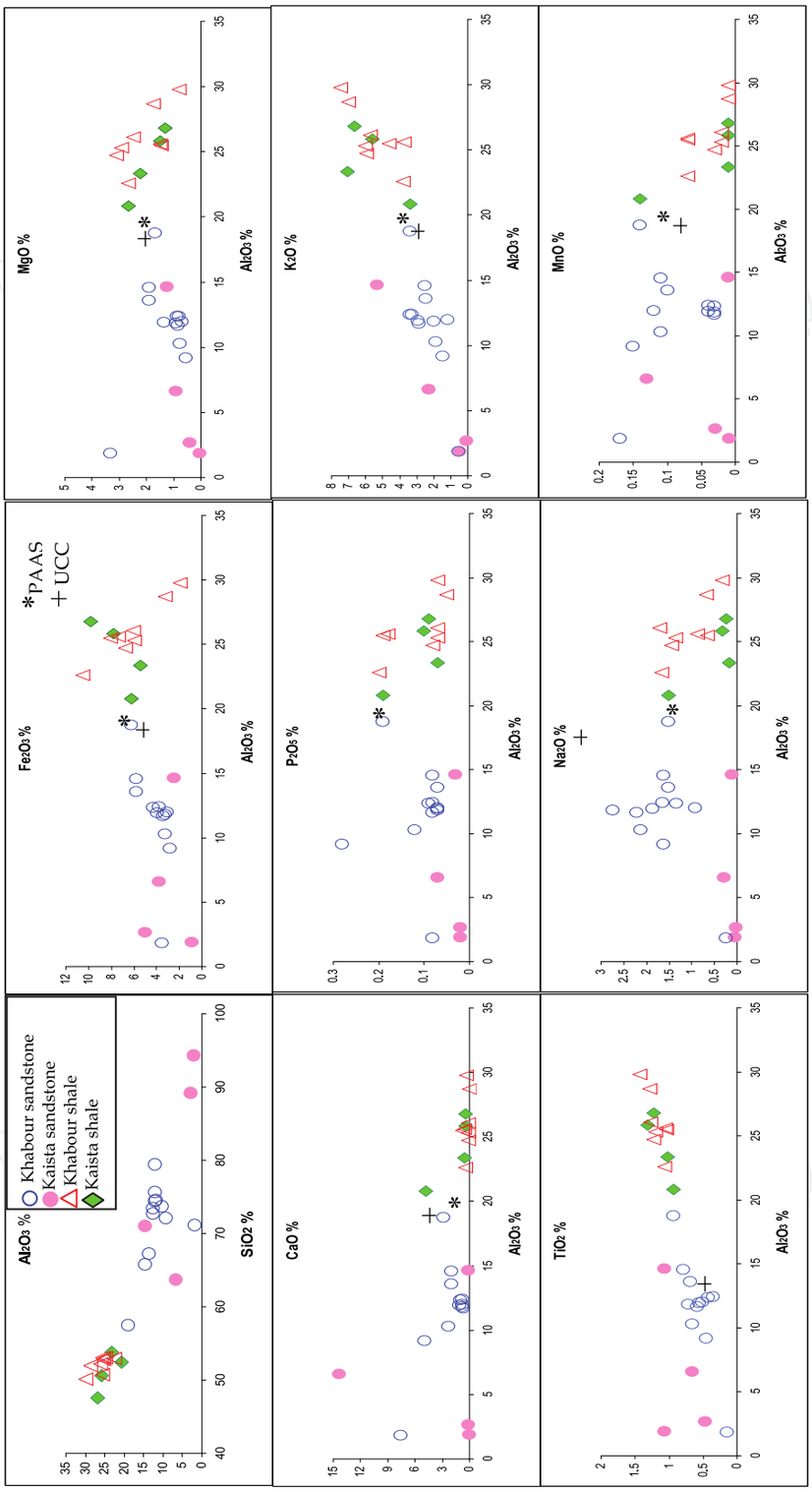

Fig. 7. Major elements versus Al_2O_3 graph showing the distribution of samples from the khabour and Kaista formations. Average data of UCC and PAAS (Taylor and McLennan, 1985) are also plotted for comparison.

with UCC. Al and Ti are easily absorbed on clays and concentrate in the finer, more weathered materials (Das et al., 2006). K_2O enrichment relates to presence of illite as common clay mineral in the studied shales (Fig. 9). On average, the studied shales have lower SiO_2 abundances relative to UCC therefore the observed variations are may be due to quartz dilution effect (Bauluz et al., 2000; Dokuz and Tanyolu, 2006).

4.2.2 Trace elements

4.2.2.1 Large ion lithophile elements (LILE): Rb, Ba, Sr, Th, and U

On average, except Rb all studied sandstones and shales are depleted in Ba, Sr, while they have higher content of Th, and U as compared with UCC (Fig. 8). Th and U show similar

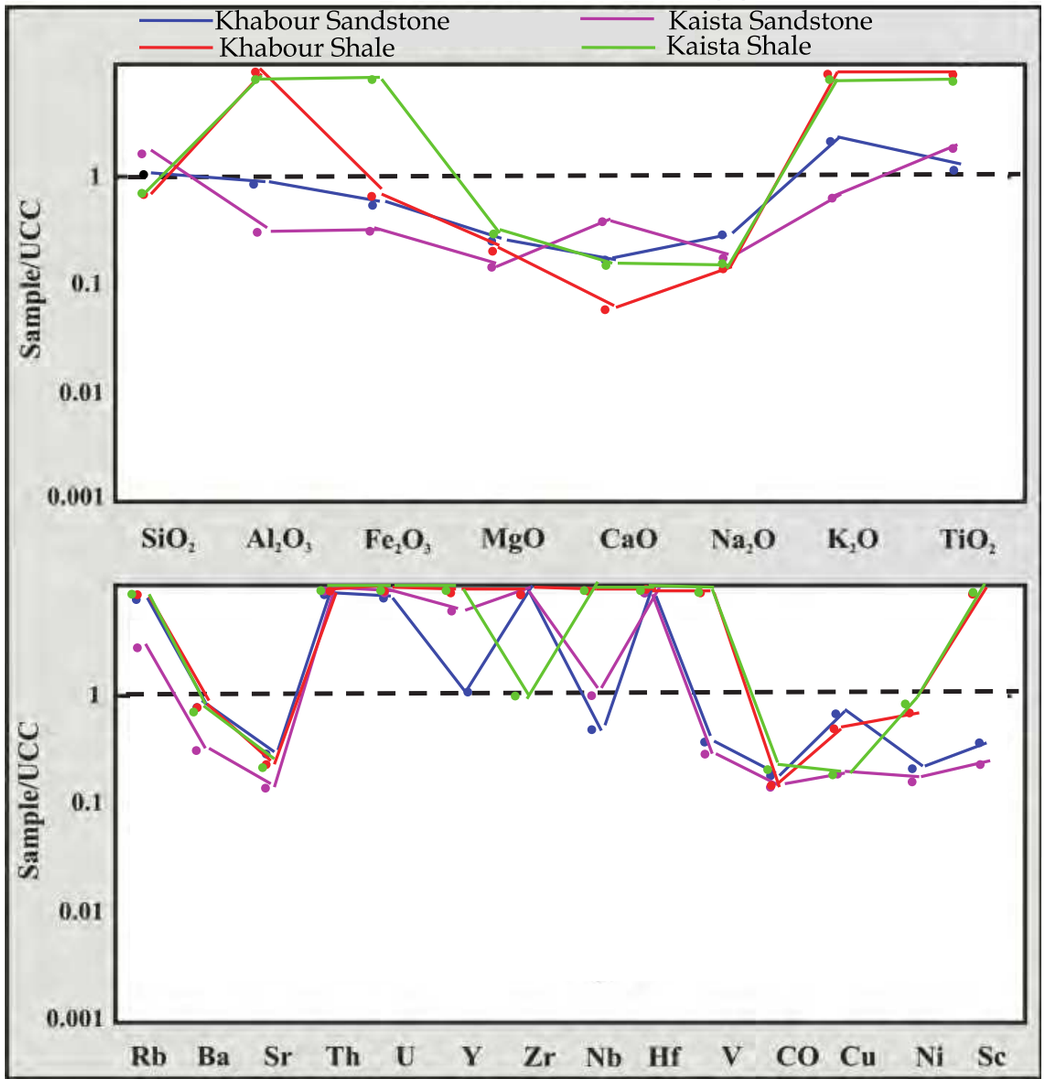

Fig. 8. Spider plot of major and trace elements composition for the Khabour and Kaista sandstones and shales normalized against UCC (Taylor and McLennan, 1985). The trace elements ordered with the large ion-lithophile (LILE) on the left (Rb-U), followed by high field strength elements (HFSE) on the right (Y-Hf) and the transition metals (V-Sc).

geochemical behavior due to their high positive correlation coefficient (r = 0.65; n=16 and r = 0.7; n=12) for sandstones and shales respectively. Except for U and Th, the remaining LILE of the studied Khabour and Kaista sandstones have significant correlations with Al_2O_3. The trace elements such as Sr, Rb, and Ba are correlated positively (r = 0.50, r = 0.60 and r = 0.73, respectively; n=28) against Al_2O_3. These correlations suggest that their distribution is mainly controlled by phyllosilicates. Th weak positive correlation with Al_2O_3 but have strong positive correlations with other elements, such as Ti and Nb (r = 0.72 and r = 0.76, respectively; n=28), implying that it may be controlled by clays and/or other phases (e .g. Ti- and Nb-bearing phases) associated with clay minerals. Rb and Ba are strong positively correlated (r = 0.89; n=16) in sandstones indicating a similar geochemical behavior, and they are also well correlated with K_2O (r = 0.90 and r = 0.89, respectively; n=16). These correlations suggest that their distributions are mainly controlled by illites.

4.2.2.2 High field strength elements (HFSE): Y, Zr, Nb, and Hf

The HFSE elements are enriched in felsic rather than mafic rocks (Bauluz et al., 2000). The concentrations of relatively all HFSE are much higher than UCC (Fig. 8). The well positive correlations for the studied sandstones obtained for TiO_2 with Zr (r = 0.59; n=20), Nb (r = 0.78; n=16), and Hf (r = 0.63; n=16) suggest that their behavior is mainly controlled by the detrital heavy mineral fraction. Zr and Hf behave similar as showed by their high positive correlation coefficient value (r = 0.90; n=16). The Zr/Hf ratio in the analyzed samples ranges from ~ 25-45. This suggests that these elements are controlled by zircons, since these values are nearly identical to those reported by Murali et al. (1983) for zircon crystals. Mean Zr content in shales are lower than the associated sandstones, which indicate that the mineral zircon tends to be preferentially concentrated in coarse-grained sands. These differences between shales and sandstones indicate that sedimentary process such as mineral sorting has played an important role.

4.2.2.3 Transition trace elements (TTE): V, Co, Cu, Ni, and Sc

TTE in the studied sandstones and shales are depleted in comparison with UCC (Fig. 8) except Sc which is more than UCC in shales. The transition trace elements do not behave uniformly. Among TTE, Sc is correlated positively with Al_2O_3 (r = 0.8; n=16) where others are well correlated in sandstones, which indicates that it is mainly concentrated in the phyllosilicates.

4.2.2.4 Rare earth elements (REE)

The ΣREE concentrations of the Khabour and Kaista sandstones are generally lower or nearly same than that of UCC. However, Khabour and Kaista shales are higher than those of UCC. Generally the studied sandstones have less content of REE than shales (ΣREE = 182.2, 281.8 and 126.0, 292.3 for the sandstones and shales of the Khabour and Kaista formation respectively). REE are generally reside in minerals like zircon, monazite, allanite, etc (McLennan, 1989). High REE in Kaista sandstones is due to high zircon content. However, the liner correlation coefficients between ΣREE and Al_2O_3 suggest that clays are also important in hosting the REE (Condie, 1991). If LREE, MREE and HREE are separately considered, all of them show positive correlations with Al_2O_3 (r = 0.48, 0.39 and 0.40, respectively; n=16) and weak positive correlation with Zr.. These positive correlations seem to indicate the variable influence of mineral phases such as phyllosilicates and less effect of zircon in controlling the REE contents.

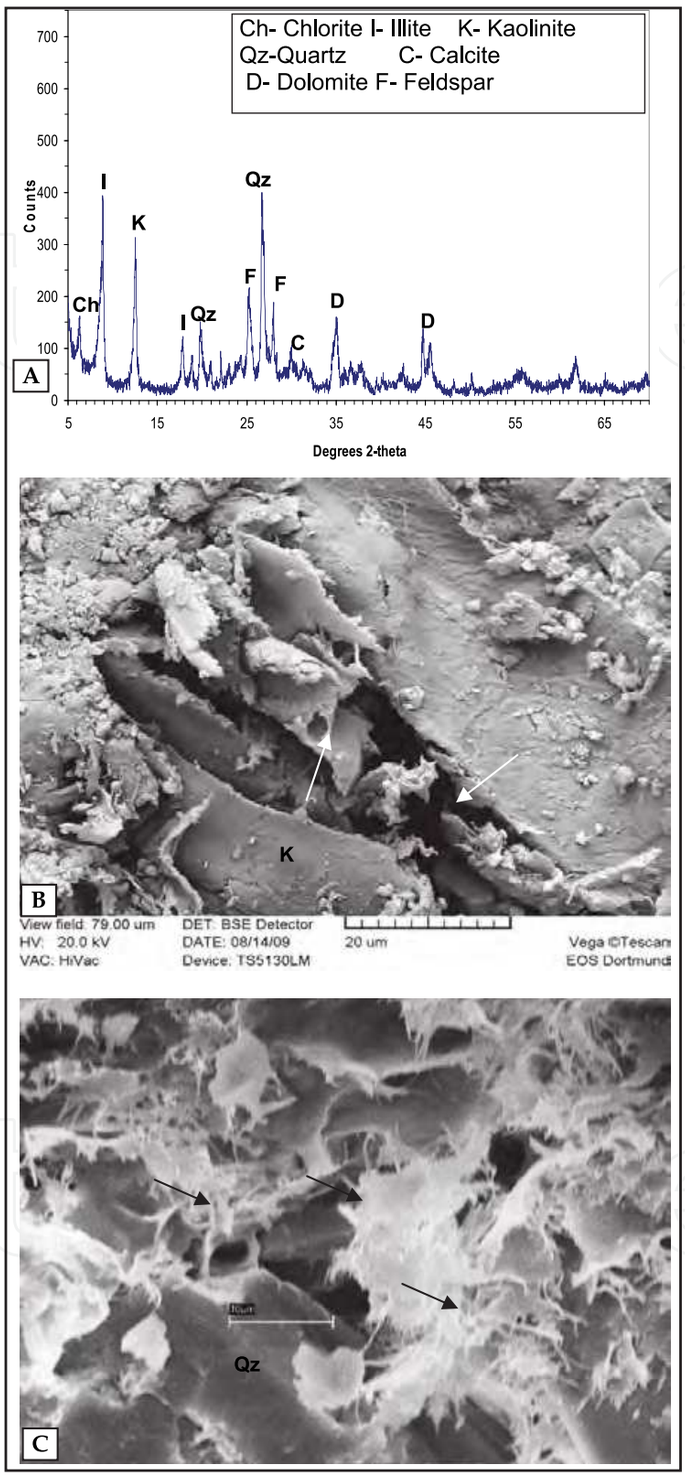

Fig. 9. A- X-Ray diffractogram showing the main clay and non-clay minerals content. B- SEM image illustrating the illite fibers (arrows) and degraded kaolinite hexagonal (K) in the Kaista shale. C- common illite fibers and flakes (arrows) filling pores in Khabour sandstone, Qz is quartz with secondary overgrowth.

Sample	S1	S2	S3	S5	S6	S8	S9	S11	Ss1	Ss3	Ss6	Ss8	Sh1	Sh3	Sh6	Sh8	Shs1	Shs2	Shs3	Shs5
SiO_2	71.2	72.8	73.5	75.7	74.6	65.9	67.3	74.5	73.8	72.2	57.5	79.5	52.9	53.1	52.8	52.2	51.9	53.0	50.7	50.1
TiO_2	0.14	0.42	0.35	0.55	0.59	0.79	0.69	0.71	0.65	0.45	0.93	0.51	1.07	1.23	1.20	1.27	1.28	1.05	1.03	1.43
Al_2O_3	1.89	12.41	12.45	11.98	11.73	14.60	13.63	11.89	10.33	9.23	18.81	12.04	22.6	24.7	25.3	26.1	28.7	25.6	25.5	29.8
Fe_2O_3	3.49	4.31	3.80	3.91	3.43	5.75	5.81	3.27	3.20	2.83	6.20	3.09	10.5	6.72	5.99	6.01	3.23	7.33	8.04	1.89
MnO	0.17	0.03	0.04	0.04	0.03	0.11	0.10	0.03	0.11	0.15	0.14	0.12	0.07	0.03	0.02	0.02	0.01	0.07	0.07	0.01
MgO	3.32	0.86	0.80	1.34	0.83	1.91	1.88	0.90	0.77	0.54	1.67	0.70	2.66	3.12	2.91	2.48	1.75	1.49	1.46	0.82
CaO	7.57	0.95	0.74	1.08	0.66	2.01	1.98	0.76	2.32	4.98	2.86	0.74	0.40	0.12	0.13	0.13	0.05	0.57	0.79	0.36
Na_2O	0.23	1.34	1.65	1.86	2.21	1.63	1.51	2.73	2.12	1.63	1.51	0.92	1.67	1.45	1.36	1.71	0.67	0.87	0.65	0.32
K_2O	0.52	3.26	3.39	2.92	2.89	2.53	2.43	2.01	1.88	1.48	3.40	1.19	3.80	5.95	6.01	5.70	6.98	3.73	4.59	7.46
P_2O_5	0.08	0.09	0.08	0.07	0.08	0.08	0.07	0.07	0.12	0.28	0.19	0.07	0.20	0.08	0.07	0.07	0.05	0.18	0.19	0.07
L.O.I.	10.9	2.89	2.71	4..90	2.49	4.51	4.04	2.78	4.48	5.29	6.35	1.12	4.23	3.80	4.03	4.41	4.74	4.98	5.97	6.87
SUM	99.51	99.36	99.51	99.45	99.54	99.82	99.44	99.65	99.78	99.06	99.58	100.0	100.1	100.3	99.82	100.1	99.36	98.87	98.99	99.13
CIA	18.5	69.0	68.3	67.1	67.1	70.3	68.8	68.4	62.0	53.3	70.8	69.5	79.4	76.7	77.1	77.6	78.8	79.9	80.9	78.5
Ni	3.3	18.7	17.9	15.3	16.2	35.0	28.3	15.2	13.5	29.0	39.9	17.7	37.9	38.5	39.3	36.4	40.0	48.9	44.2	49.3
Co	0.2	6.0	5.8	5.0	4.6	14.6	10.3	4.3	7.8	9.2	15.3	8.1	4.8	6.6	15.0	12.6	8.9	5.7	5.6	6.3
Cr	8.8	35.1	34.7	29.4	38.1	70.5	55.2	45.9	29.6	79.9	104.8	12.2	91	100.8	163.1	147.1	147.6	81.7	169.3	144.5
V	13.1	53.3	53.7	41.9	47.4	96.4	76.9	63.0	38.5	66.8	129.1	13.2	85.3	83.8	133.1	181.4	176.9	169.3	106.4	160.5
Sc	1.2	7.1	7.0	6.2	7.2	12.2	9.7	7.2	4.4	11.9	20.0	4.2	16.1	12.3	19.6	17.6	28.5	15.2	23.5	27.6
Cu	5.1	17.2	12.1	21.7	15.1	27.0	19.2	13.7	32.6	30.7	27.1	18.4	39.5	23.5	20.7	29.6	18.3	7.1	11.3	2.8
Zn	223.1	65.1	63.5	134.5	53.3	90.4	86.5	79.6	108.5	99.4	80.7	309.5	73.2	81.4	65.7	51.9	37.7	204.4	57.6	24.0
Pb	12.4	36.8	53.8	35.4	29.1	23.1	20.2	26.5	17.4	12.4	36.9	38.8	8.3	14.3	14.6	10.9	12.5	24.7	53.4	9.7
Sr	70.4	193.3	217.9	203.2	203.4	166.1	175.3	325.6	249.0	70.4	193.4	49.0	177	162	187	224	128.3	120.5	139.6	116.1
Rb	15.7	97.1	100.7	81.1	83.7	99.9	69.5	47.7	134.9	15.7	96.7	12.0	257.1	141.4	176.3	210.1	149.8	153.0	147.9	195.8
Ba	91.2	689.8	700.3	653.6	654.3	448.0	472.6	358.1	765.2	91.2	689.9	122.2	1014	622	657	1316	231	433	831	649
Zr	140.1	179.0	111.4	509.4	415.1	223.4	511.8	488.6	240.6	140.1	178.8	155.5	215.3	176.0	230.3	300.8	318	184	835	282
Hf	4.1	5.1	3.2	12.1	10.0	6.2	13.1	9.2	6.5	13.0	9.3	5.4	5.3	4.2	6.1	9.1	9.4	7.2	19.1	8.1
Nb	2.7	8.9	7.5	10.3	11.3	17.4	15.4	9.6	21.0	2.7	8.9	4.2	26.3	19.1	20.4	27	34.3	21.8	272	35.2
Ta	2.5	1.0	1.9	2.1	2.0	2.3	2.6	2.9	2.5	2.5	1.4	2.4	1.0	0.9	1.1	1.7	3.3	3.4	2.9	3.1
Th	2.4	7.4	6.5	12.5	11.3	11.8	12.9	12.1	17.3	2.4	7.4	19.8	23.5	12.9	14.7	22.9	27.3	16.4	26.0	31.3
U	1.1	1.5	1.7	2.7	2.6	2.7	3.3	2.9	3.9	1.1	1.5	1.0	0.9	0.9	0.9	1.6	9.5	6.6	7.8	14.6
Y	21.5	19.7	16.4	21.0	24.4	26.0	30.4	26.1	38.1	21.5	19.7	20.0	30.6	21.8	22.2	29.2	57.8	40.1	38.5	35.7
La	12.0	23.6	26.6	32.0	38.5	27.7	35.9	27.5	39.9	51.9	44.0	44.5	59.2	24.2	49.4	48.6	48.6	61.2	59.1	60.5
Ce	25.4	46.5	52.5	59.5	71.2	54.2	69.8	52.8	87.1	107.8	95.6	87.3	106.6	47.0	81.7	80.1	98.8	116.2	113.4	114.8
pr	3.0	5.4	6.1	6.7	8.1	6.2	7.9	5.8	9.7	12.1	10.7	9.9	11.8	5.3	10.4	10.3	11.1	13.0	12.3	12.5
Nd	12.3	23.7	25.6	24.0	23.3	30.5	27.1	22.0	48.6	12.3	23.7	42.8	67.4	70.2	71.4	69.6	76.8	52.0	49.7	62.7
Sm	2.1	4.7	4.4	4.9	4.8	3.8	6.2	2.7	7.7	2.1	4.7	10.1	13.2	16.7	15.3	14.2	18.1	13.0	9.1	13.3
Eu	1.0	1.2	1.2	1.2	1.2	1.1	1.1	0.9	1.7	2.1	2.1	1.9	1.7	0.6	2.0	2.0	1.9	2.0	1.7	1.6
Gd	4.8	4.6	4.5	5.2	5.4	4.6	5.4	4.4	6.8	8.6	9.4	10.1	9.2	2.7	9.0	8.9	8.5	8.2	6.9	6.7
Tb	0.9	0.9	0.7	0.9	0.9	0.8	1.0	0.8	1.1	1.5	1.6	1.9	1.7	0.5	1.6	1.6	1.4	1.4	1.2	1.1
Dy	4.1	4.0	3.5	4.0	4.7	4.3	5.1	4.3	4.9	7.6	8.0	8.9	9.2	2.8	8.4	8.3	7.0	7.0	6.4	5.5
Ho	0.8	0.8	0.6	0.8	0.9	0.9	1.0	0.8	0.9	1.6	1.6	1.7	1.9	0.6	1.8	1.8	1.4	1.4	1.4	1.2
Er	1.9	2.4	1.8	2.3	2.6	2.4	3.1	2.5	2.5	4.4	4.3	4.6	5.1	1.8	5.1	4.9	3.7	4.0	4.0	3.4
Tm	0.3	0.3	0.3	0.3	0.4	0.4	0.5	0.4	0.4	0.7	0.6	0.7	0.8	0.3	0.8	0.8	0.6	0.6	0.6	0.5
Yb	1.8	2.0	2.1	2.3	2.9	2.8	3.5	2.7	4.6	4.7	4.6	2.3	5.5	1.9	5.5	5.4	4.0	4.5	4.6	4.0
Lu	0.2	0.3	0.2	0.3	0.4	0.4	0.5	0.4	0.3	0.6	0.6	0.7	0.7	0.3	0.8	0.8	0.6	0.6	0.7	0.9

Table 2. Major and trace elements concentration of selected Khabour sandstone (S and Ss) and shale (Sh) samples. (See Figure 2 for samples location)

Sample	KS1	KS2	KS3	KS4	KSh1	KSh2	KSh3	KSh4
SiO_2	94.43	89.26	71.11	63.82	50.58	47.53	53.78	52.5
TiO_2	1.07	0.46	1.06	0.65	1.32	1.23	1.02	0.93
Al_2O_3	1.93	2.71	14.68	6.65	25.84	26.80	23.36	20.81
Fe_2O_3	0.88	4.99	2.45	3.80	7.83	9.81	5.41	6.20
MnO	0.009	0.029	0.01	0.13	0.01	0.01	0.01	0.14
MgO	0.04	0.40	1.25	0.92	1.51	1.31	2.23	2.67
CaO	0.03	0.08	0.14	14.32	0.41	0.43	0.54	4.86
Na_2O	0.04	0.03	0.11	0.28	0.32	0.24	0.18	1.51
K_2O	0.49	0.05	5.29	2.27	5.60	6.68	7.08	3.40
P_2O_5	0.02	0.02	0.03	0.07	0.10	0.09	0.07	0.19
L.O.I.	0.34	1.07	3.37	6.79	6.12	5.29	5.80	6.35
SUM	99.28	99.1	99.5	99.7	99.64	99.42	99.48	99.56
CIA	77.5	91.9	28.6	29.3	80.3	78.5	75.0	68.1
Ni	6.1	22.2	19.8	9.4	48.9	61.9	49.1	39.9
Co	1.1	11.9	2.0	3.5	7.5	8.3	13.8	15.3
Cr	38.0	20.7	86.5	37.2	120.0	129.2	126.5	104.8
V	38.5	15.6	93.1	58.5	124.5	149.8	175.6	129.1
Sc	2.7	1.7	15.6	5.5	25.1	20.9	22.4	20.0
Cu	9.8	7.7	3.4	9.5	3.5	3.7	4.0	27.1
Zn	4.6	22.7	21.5	21.7	71.4	55.7	60.9	80.7
Ga	2.2	2.9	22.4	9.1	28.7	27.7	32.1	13.7
Pb	14.6	8.9	5.2	7.3	12.1	16.6	9.0	36.9
Sr	23.6	28.5	40.5	147.9	108.8	161.3	69.1	193.4
Rb	10.5	2.5	224.3	85.6	184.4	189.5	271.0	96.7
Ba	29.0	31	895	295	542	542	467	495
Zr	1115	343	445	668	306	226	128	178.8
Hf	31	8.0	12	15	8	6	5	9
Nb	21.5	8.9	28.9	14.5	30.0	31.5	27.1	8.9
Ta	2.8	2.0	3.5	1.2	2.4	3.3	2.7	1.4
Th	22.9	9.4	22.5	12.8	27.1	24.2	21.8	7.4
U	4.1	2.1	3.0	1.8	6.0	4.8	5.3	1.5
Y	30.3	15.4	21.5	33.1	38.2	51.8	22.4	19.7
L.a	16.2	21.1	34.1	34.5	31.7	92.1	44.9	100.1
Ce	31.0	42.7	64.2	63.8	55.5	170.1	76.4	193.8
Pr	3.7	5.5	6.7	7.6	6.1	18.1	8.2	20.4
Nd	14.3	23.7	24.3	31.2	22.6	75.0	29.6	84.5
Sm	2.1	5.1	3.4	6.2	3.8	14.2	4.3	15
Eu	3.0	1.0	0.6	1.0	0.8	2.9	0.8	2.7
Gd	0.5	4.5	2.9	5.3	3.5	10.8	3.8	10.9
Tb	2.9	0.8	0.6	1.0	0.7	1.8	0.7	1.6
Dy	0.5	3.8	3.2	4.9	4.0	8.8	3.8	6.9
Ho	2.7	0.7	0.7	1.0	0.9	1.7	0.8	1.3
Er	1.6	2.0	2.4	2.8	2.7	4.8	2.5	3.7
Tm	0.2	0.3	0.4	0.4	0.4	0.7	0.4	0.6
Yb	1.6	1.9	3.0	3.1	3.2	5.2	2.9	4.2
Lu	0.2	0.3	0.5	0.4	0.5	0.8	0.5	0.5

Table 3. Major and trace elements concentration of selected sandstone (KS) and shale (KSh) samples of the Kaista Formation (See Figure 3 for samples location)

5. Provenance information from sandstones

5.1 Source rocks

As pointed out above, sandstones petrographic investigation revealed that they are variable (Table 1) with detrital quartz being the most abundant and constant component. The average quartz content of the Khabour sandstones is 63% and 65% for the Kaista sandstones. The feldspar content range from 6% to 12 %, and from 2% to 3% in the Khabour and Kaista sandstones respectively. Rock fragments range from 1 % to 9% in the Khabour sandstones and from 1% to 7% in the Kaista sandstones with sedimentary rock fragments dominated by chert being the dominant and small and occasional content of igneous and metamorphic fragments.

The qualitative petrography study provides important information on the nature of the source area. Mono-crystalline quartz is the most abundant framework grains. Whereas, few polycrystalline quartz grains of (> 3 grains) per each polycrystalline grain were identified. Most of monocrystalline quartz grains are of straight to slightly undulatory extinction, with or without inclusions; where present, the most common inclusions are vacuoles, acicular rutile, spherulitic zircon, muscovite, apatite and iron oxides. Quartz types, inclusions and undulosity indicate a derivation from a dominantly plutonic (granitic) provenance with subordinate input from low rank metamorphic rocks. (Basu et al., 1975).

to discriminate provenance fields for the studied rocks, a TiO_2 vs. Ni bivariate plot (Fig. 10; Floyd et al., 1989) is used. The majority of samples plot in the acidic field, even though few samples plot outside the field assigned for felsic source.

On a the La/Th vs. Hf bivariate (Fig. 11; Floyd and Leveridge, 1987) suggests the felsic source rocks although there are some differences in source rocks between shales and sandstones. Furthermore, La/Sc versus Th/Co bivariate diagram (Fig. 12; Cullers, 2002), shows that nearly all the studied samples plot near to the silicic rock provenance composition. In addition, the REE patterns and the size of the Eu anomaly have been also used to infer sources of sedimentary rocks (Taylor and McLennan, 1985). Since basic igneous rocks contain low LREE/HREE ratios and little or no Eu anomalies, whereas silicic igneous rocks usually contain higher LREE/HREE ratios and negative Eu anomaly (Cullers, 1994; Cullers et al., 1987). The average chondrite normalized REE patterns of the studied rocks are shown in Figure 13.

For comparison average REE patterns of Continental Crust , Continental Arc, Mid-Oceanic Ridge, and Oceanic Island Basalt are also included in this Figure 13. The chondrite normalized REE patterns for the Khabour and Kaista sandstones and shales are comparable to Continental Crust and Continental Arc. The REE patterns suggest that the samples were mainly derived from an old upper continental crust composed chiefly of felsic components. Similarly, in the Eu/Eu* and Th/Sc plot (Fig. 14; Cullers and Podkovyrov, 2002) the samples plot between the average values of granite and granodiorite source rocks with rare mafic provenance.

The post-Archean pelites have low concentrations of mafic elements, particularly Ni and Cr, when compared to Archean pelites (McLennan et al., 1993). The reason for the high concentrations of Ni and Cr in the Archean pelites is due to the deficiency of ultra-mafic rocks in the post Archaean Period (Taylor and McLennan, 1985). The studied sandstones plot in the post Archaean field (Fig. 15) and suggest that the felsic component was dominant in the source area of the Khabour and Kaista formations. The (Gd/Yb)CN ratio also

document the nature of source rocks and the composition of the continental crust (Nagarajan et al., 2007; Taylor and McLennan, 1985). On a Eu/Eu* vs. (Gd/Yb)CN diagram (Fig. 16), the studied shales and most of the sandstones plot in the post Archean field and near to PAAS value, which suggest that the post Archean felsic rocks could be the source rocks for the Khabour and Kaista formations. Archean sources could be compared with those sources recorded for Paleozoic clastics in southern Turkey (Kröner and Sengör, 1990) and Iran (Etemad Saeed etal., 2011).

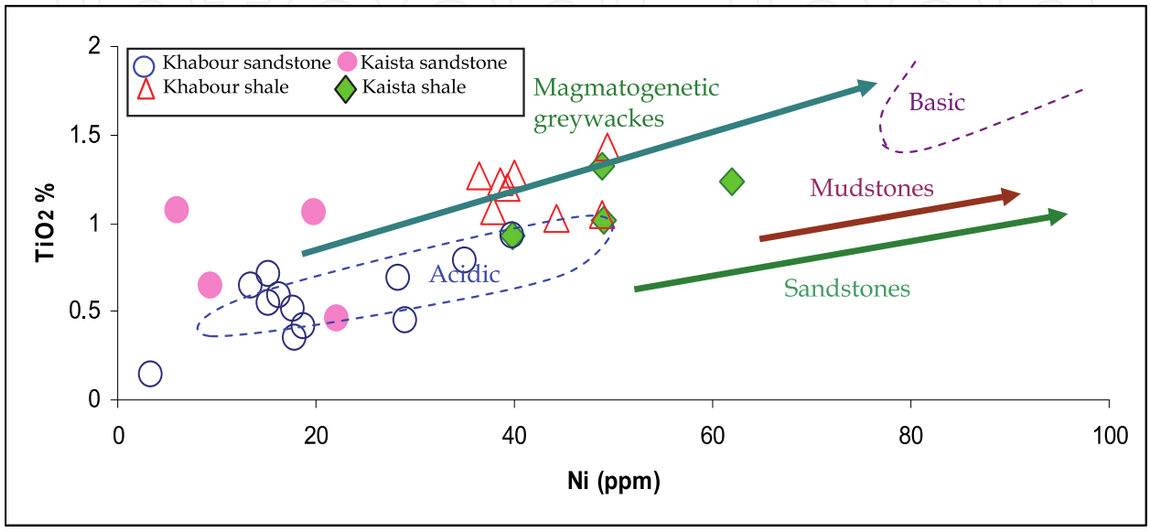

Fig. 10. TiO_2 versus Ni bivariate plot for the studied sandstones (Floyd et al., 1989). Majority of samples plot near the acidic sources.

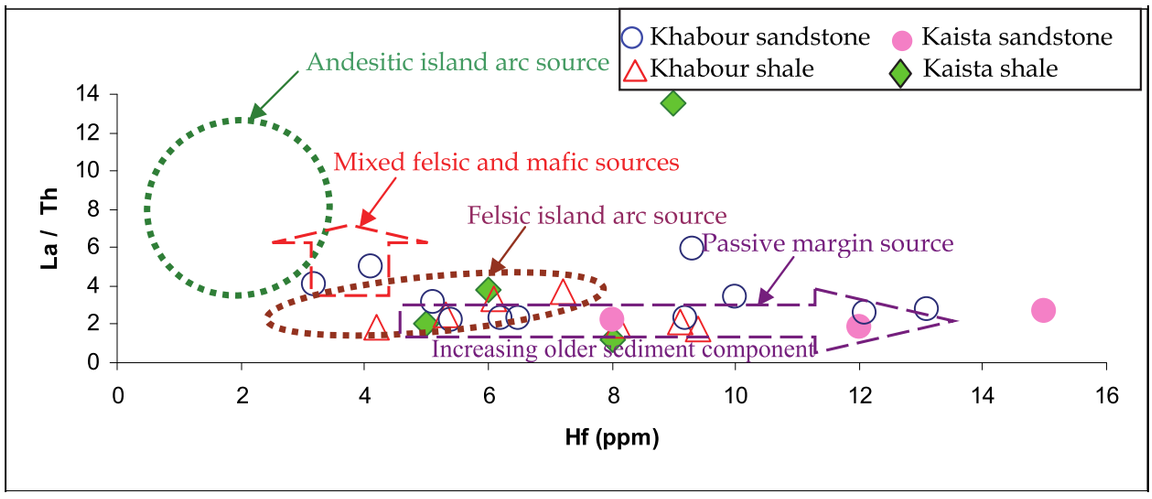

Fig. 11. Hf versus La/Th diagram (Floyd and Leveridge, 1987).

McLennan et al. (1990) recognized four distinctive provenance components on the basis of geochemistry: old upper continental crust, young undifferentiated arc, young differentiated (Intracrustal) arc and Mid-Ocean ridge basalt (MORB). This study reveals that the studied

sandstones and shales were derived from an old and well-differentiated upper continental crust provenance, which is characterized by high abundances of large ion lithophile (LILE) elements, high Th/Sc, La/Sm, Th/U ratios and negative Eu anomaly (McLennan et al., 1990). It seems that the felsic source for the Khabour and Kaista formations are similar to the

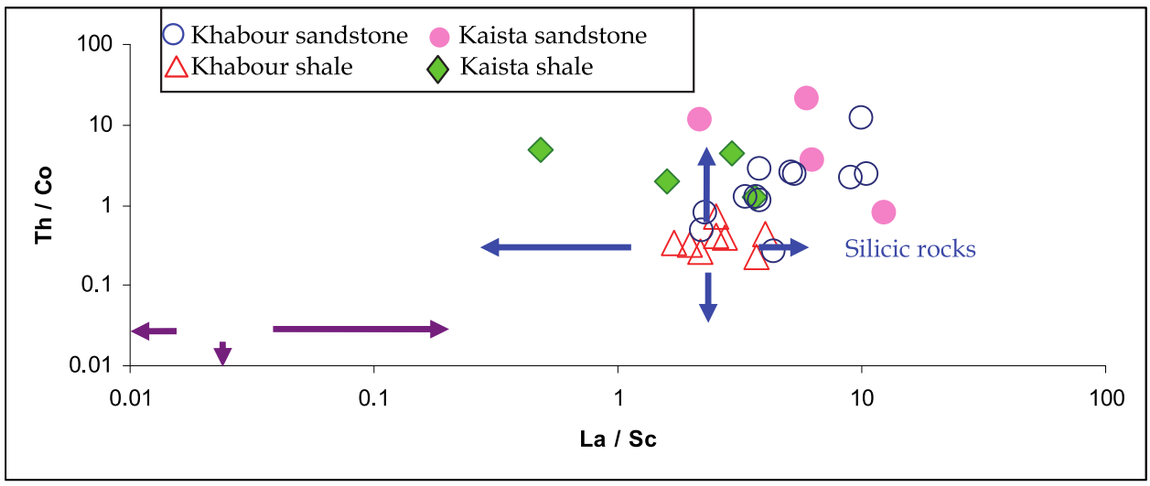

Fig. 12. Th/Co versus La/Sc plot (Cullers, 2002). The studied sandstones and shales plot near the silicic source.

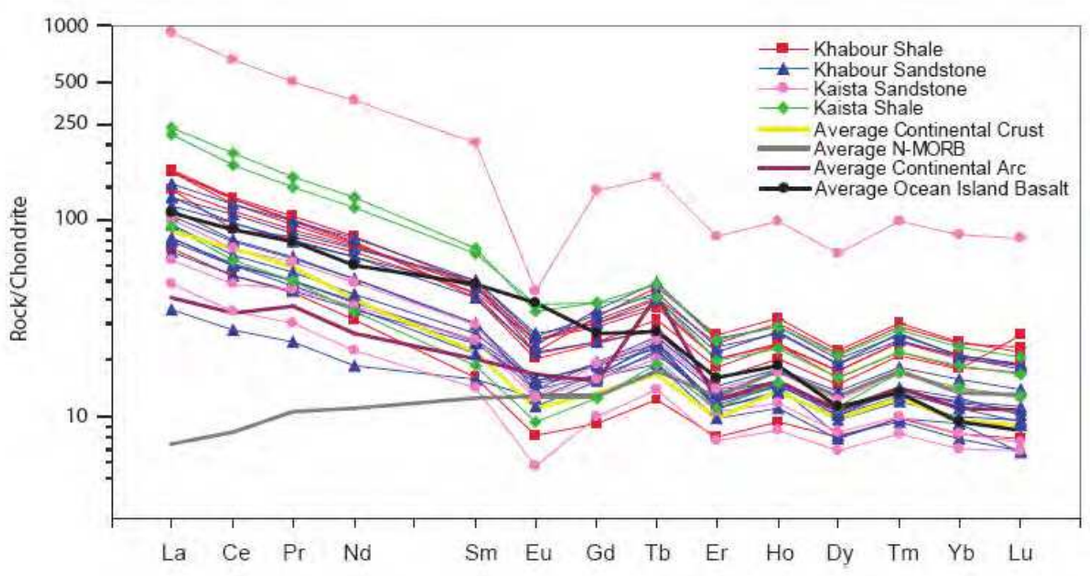

Fig. 13. Chondrite normalized rare earth element plots for the studied sandstones and shales. Average Continental Crust , Continental Arc, Mid-Oceanic Ridge, and Oceanic Island Basalt are also included. Data sources: Average Upper continental crust (Taylor and McLennan, 1995), N-MORB (average Sun and McDonough 1989) Continental arc (average from Georoc database query basaltic andesite convergent margin, ICPMS, REE only), Ocean Island basalt (Sun and McDonough 1989)

acidic and basic igneous basement rocks of Iraq. The crystalline basement rocks of Iraq is interpreted from seismic and geophysical data to range in depth from about 6–10 km and is composed mostly of granitic, basic and ultra basic igneous and metamorphic rocks (Buday, 1980; Al-Hadidy, 2007).

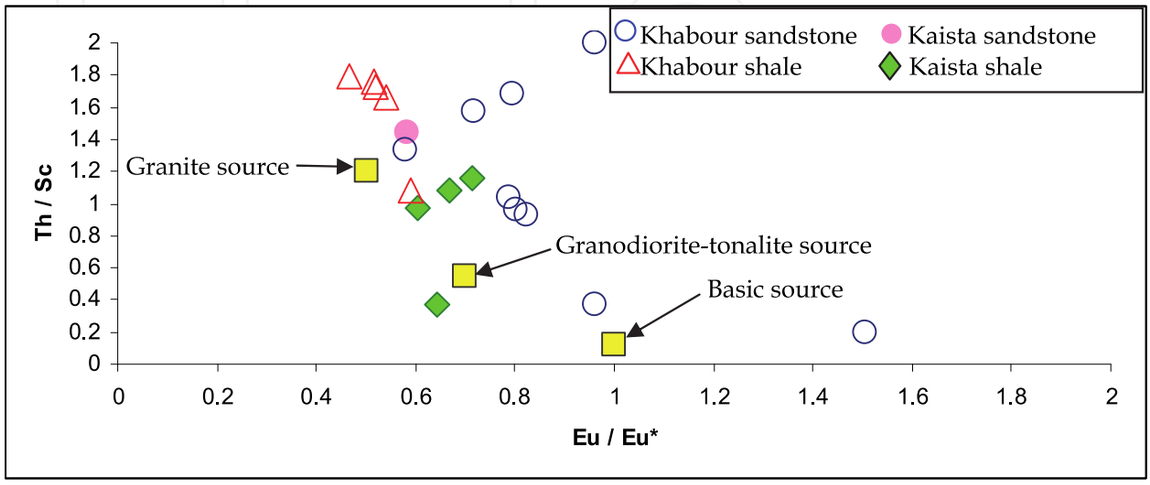

Fig. 14. Eu/Eu*-Th/Sc bivariate plot for the samples from the Khabour and Kaista formations (Cullers and Podkovyrov, 2002).

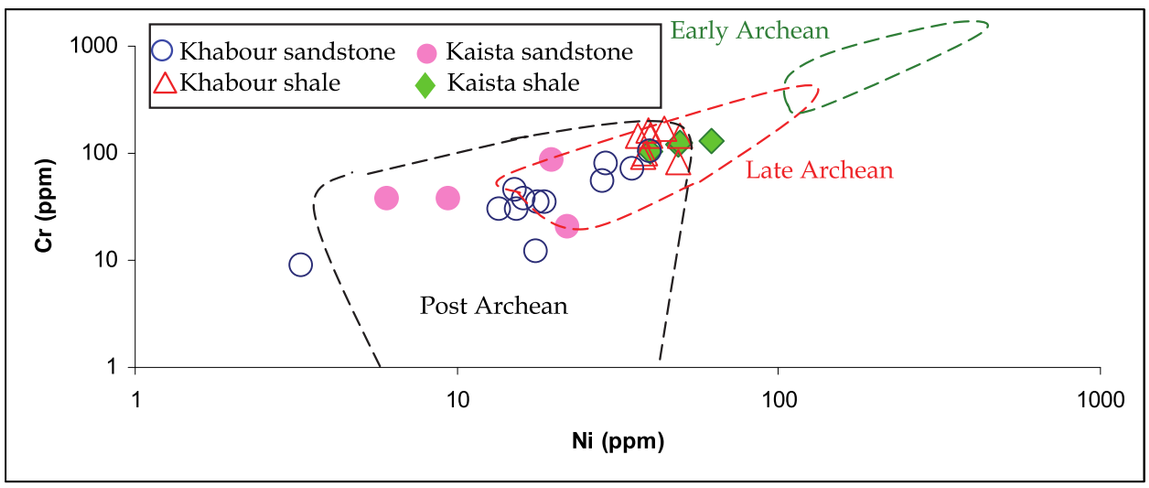

Fig. 15. Ni-Cr bivariate plot for the samples from the Khabour and Kaista formations (McLennan et al., 1993).

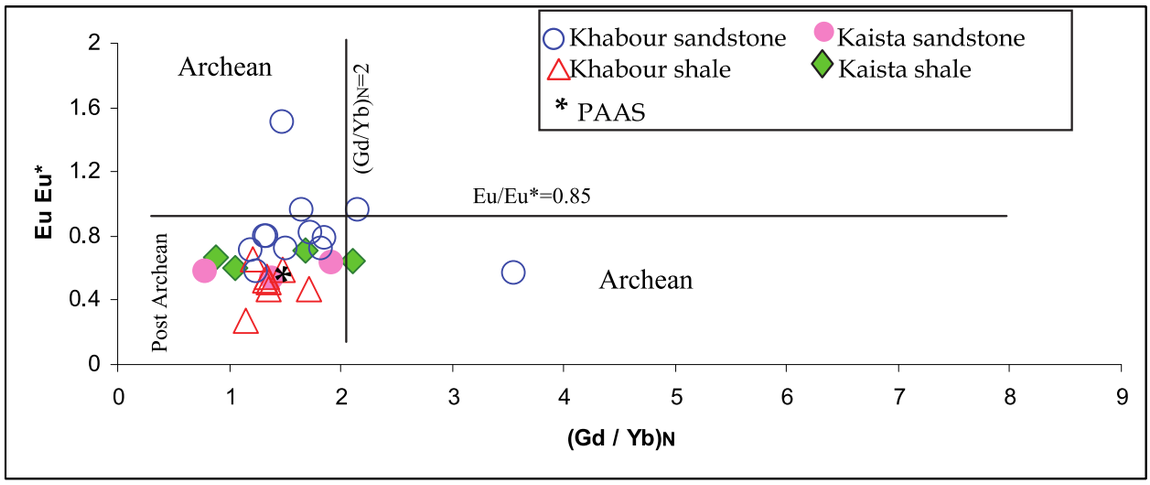

Fig. 16. Plot of Eu/Eu* versus (Gd/Yb)CN for the samples of the studied formations. Fields are after McLennan and Taylor (1991).

5.2 Implications for tectonic setting

Petrographic data from various framework constituents (Quartz, Feldspar, and Rock Fragments) were plotted on various ternary and bivariate diagrams to show their positions on various schemes in order to discriminate their tectonic settings and show their paleoclimatic and weathering conditions. On the Qt-F-L and Qm-F-Lt diagrams (Figure 17A) of Dickinson and Suczek, (1979), the Khabour sandstones plot in the recycled orogen and continental block provenances with stable craton sources and with uplifting in the basement complexes. Whereas, Kaista sandstones were plotted in the recycled Orogen Provenance. Similarly, in the Lm-Lv-Ls and Qp-Lvm-Lsm ternary diagrams of Ingersoll and Suczek (1979) (Figure 17B) the studied sandstones plot mostly in mixed arc and subduction continental margin and in rifted continental margins and partly in sutured belt provenances.

Within recycled orogens, sediment sources are dominantly sedimentary with subordinate volcanic rocks derived from tectonic settings where stratified rocks are deformed, uplifted and eroded (Dickinson, 1985; Dickinson and Suczek, 1979). As pointed out by Dickinson et al. (1983), sandstones plotting in craton interior field are mature sandstones derived from relatively low-lying granitoid and gneissic sources, supplemented by recycled sands from associated platform or passive margin basins. The detrital modal compositions of both Khabour and Kaista sandstones are plotted in the Q-F-L diagram (Fig. 18; Yerino and Maynard, 1984), which indicates that these sandstones are related to trailing-edge margin. Bhatia (1983) and Roser and Korsch (1986) proposed tectonic setting discrimination fields for sedimentary rocks to identify the tectonic setting of unknown basins. These tectonic setting discrimination diagrams are still extensively used by many researchers to infer the tectonic setting of ancient basins (Drobe et al., 2009; Gabo et al., 2009; Maslov et al., 2010; Wani and Mondal, 2010 Bakkiaraji et al., 2010; Bhushan and Sahoo, 2010; de Araújo et al., 2010). However, the functioning of major elements tectonic setting discrimination diagrams proposed by Bhatia (1983) and Roser and Korsch (1986) have been evaluated in many studies. Armstrong-Altrin and Verma (2005) observed that the tectonic setting discrimination diagram proposed by Roser and Korsch (1986) works better than Bhatia's

(1983) diagram. In this study, K_2O/Na_2O versus SiO_2 tectonic setting discrimination diagram (Fig. 19) shows that most of the Khabour and Kaista samples fall in the Active continental and passive margin fields.

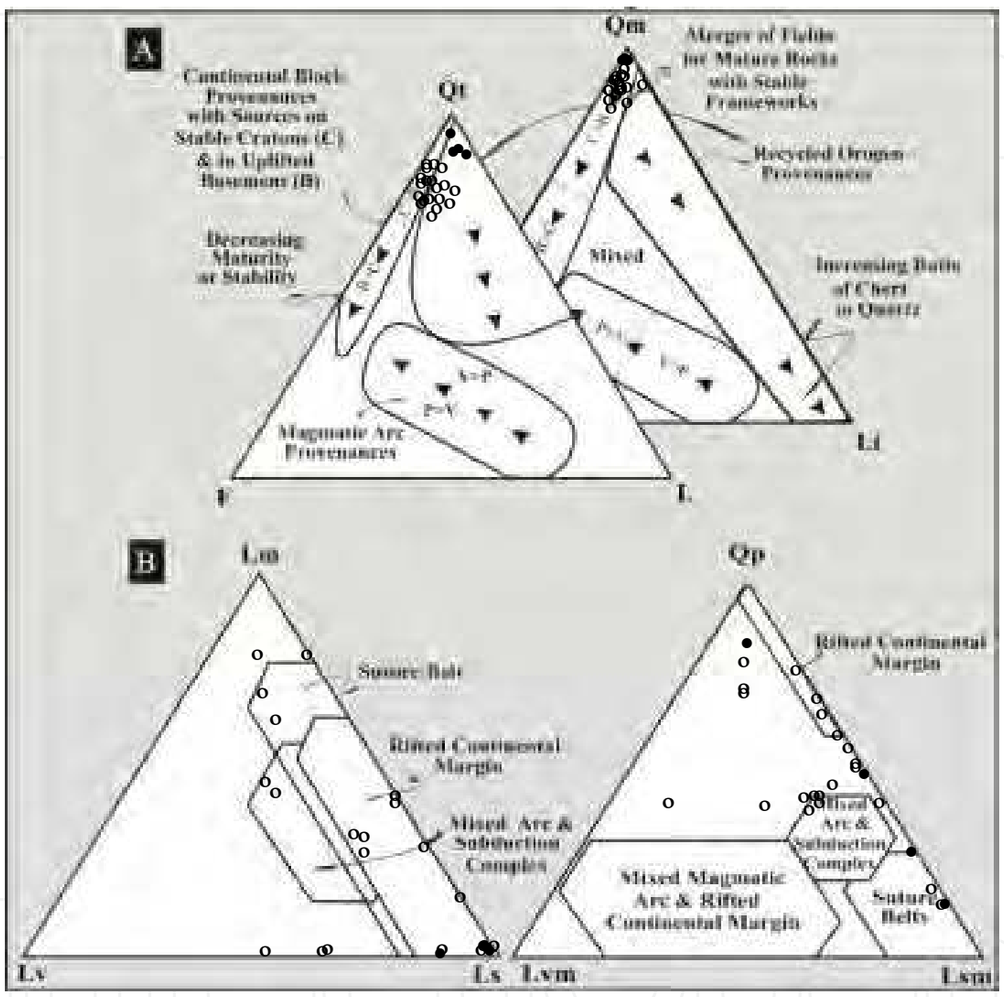

Fig. 17. Provenance diagrams for the studied sandstones (A) Qt-F-L and Qm-F-Lt plots.Tectonic setting fields after Dickinson and Suczek (1979), and (B) Lm-Lv-Ls and Qp-Lvm-Lsm after Ingersoll and Suczek (1979). Data and definitions are given in Table 1.

As discussed above, the Khabour and Kaista sandstones posses similar characteristics of a passive margin setting as described by McLennan et al. (1993). Passive margin sediments are largely quartz-rich, derived from plate interiors or stable continental margins. Bhatia (1983) opined that the sedimentary rocks deposited on passive margins are characterized by enrichment of LREE over HREE with pronounced negative Eu anomaly on chondrite-normalized patterns.

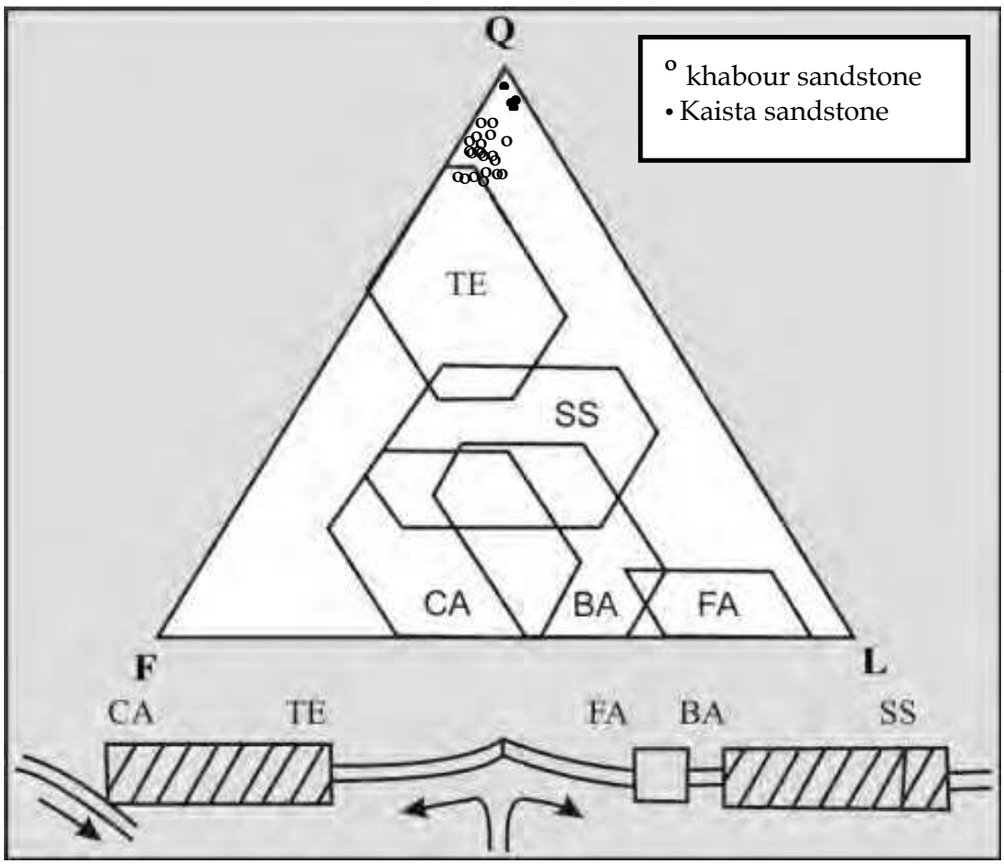

Fig. 18. Q-F-L tectonic provenance diagram for the Khabour and Kaista sandstones, after Yerino and Maynard (1984). The studied sandstones plot near the TE field. TE: trailing edge (also called passive margin); SS: strike-slip; CA: continental-margin arc; BA: back arc to island arc; FA: fore arc to island arc.

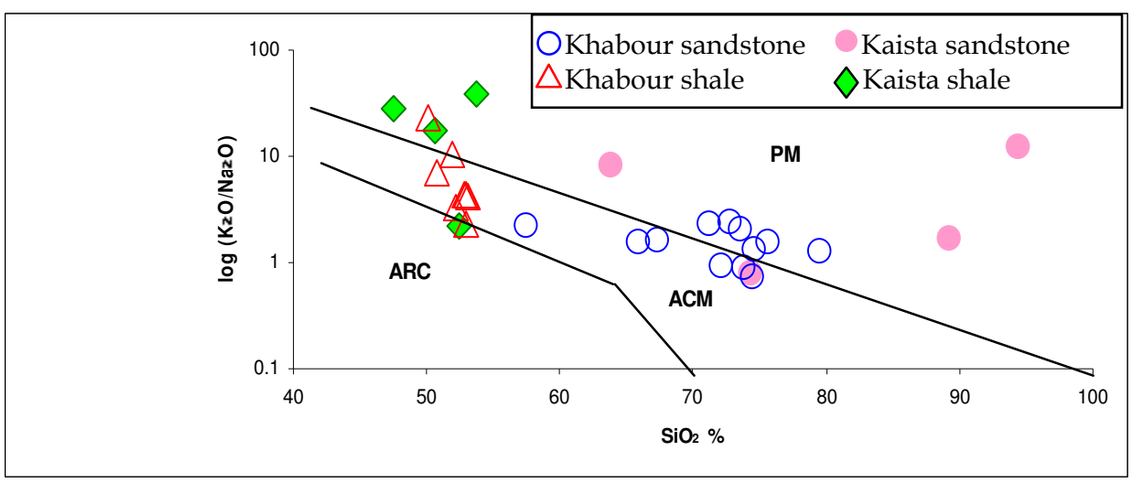

Fig. 19. Tectonic-setting discrimination diagram after Roser and Korsch (1986). PM = passive margin; ACM = Active continental margin; ARC = Island arc.

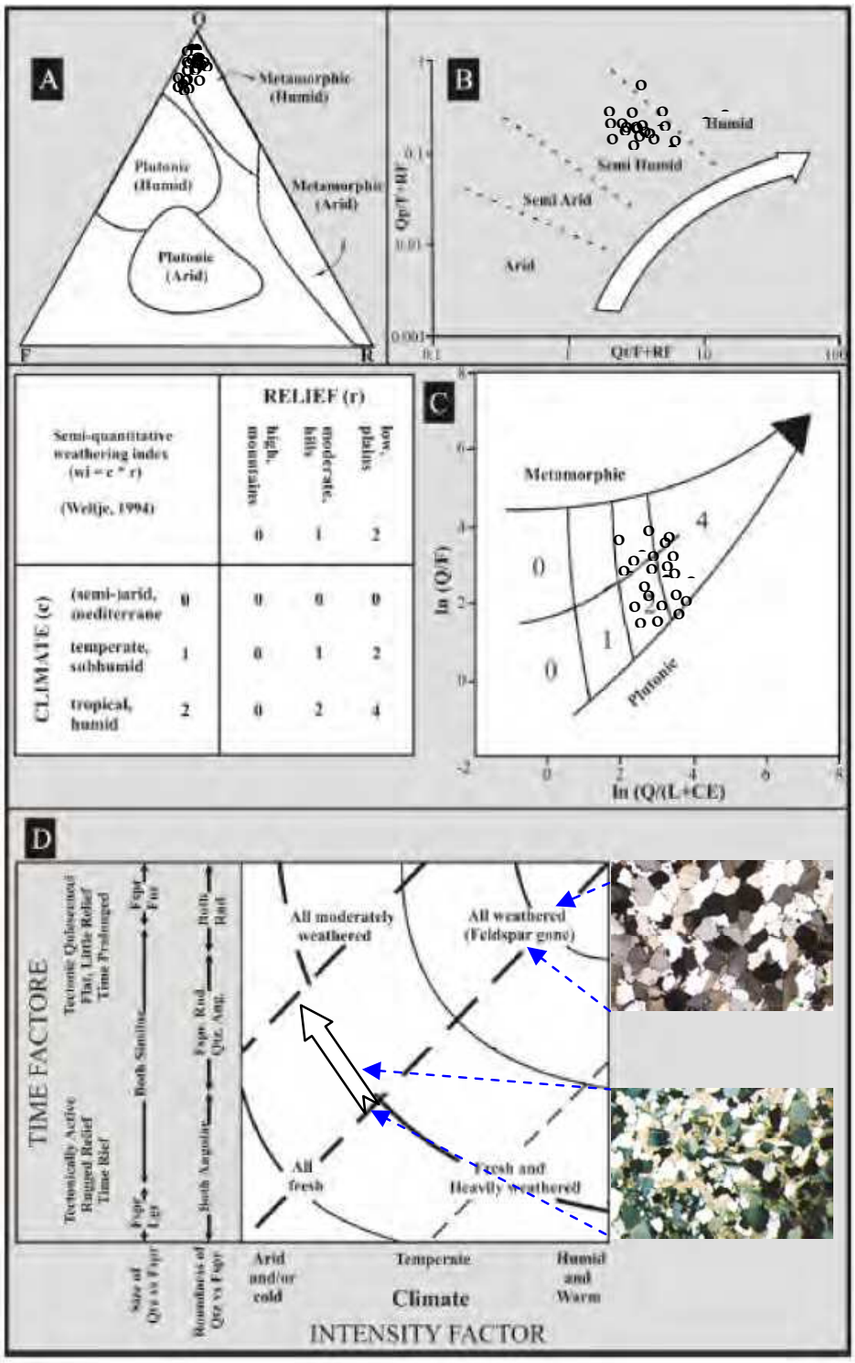

Fig. 20. Illustrating the effect of climate on the composition of the Khabour sandstones using, A- Suttner et al., (1981) diagram. Q:Quartz; F: Feldspar, R: Rock fragments. B- Bivariate log/log plot (Suttner and Dutta, 1986). Qt: total Quartz, F: Feldspar, RF: Rock fragments, Qp: Polycrystalline quartz. C- Weathering diagram and semi-quantitative weathering index after Weltje (1994). CE: Carbonate clasts. D- Evaluate of paleoclimate condition based on relation between quartz and feldspar grains and degree of weathering of feldspar grains (Folk, 1974).

5.3 Weathering, relief, and climate

In the Q-F-R ternary diagram (Suttner et al., 1981), Khabour and Kaista sandstones plot in the field of the metamorphic source area with humid climate (Fig. 20A). In addition, in the bivariate diagram of Suttner and Dutta (1986) the studied sandstones reveal the differences in climate condition from semi-arid to humid (Fig. 20B). Similarly, in the Grantham and Velbel (1988) weathering index wi = c* r and Weltje (1994) diagrams (Fig. 20C), the studied sandstones plot into the field of wi = 2 and 4 indicating moderate to high degree of weathering in low plains relief and from semi-arid to semi-humid climate conditions and mainly between metamorphic and plutonic compositions. Furthermore, in the Folk (1974) weathering intensity diagram (Fig. 20D), some of the Khabour and Kaista sandstones plot in the mixed moderately weathered field and fresh feldspars plot in the temperate to arid climate field, whereas quartzite sandstones of both formations plot in the humid climate field. The intensity and duration of weathering in clastic sediments can be evaluated by examining the relationships among alkali and alkaline rare earth elements (Nesbitt and Young, 1996; Nesbitt et al., 1997). Various investigators have utilized the so-called "Chemical Index of Alteration" (CIA) of Nesbitt and Young (1982) to evaluate the intensity and the degree of chemical weathering: CIA = $[Al_2O_3/(Al_2O_3 + CaO + Na_2O + K_2O)] * 100$, where the oxides are expressed as molar proportions and CaO represents the Ca in silicate fractions only. The high CIA values in shales (mean 79 and 76, for the Khabour and Kaista formations respectively) and most of the studied sandstones (see Tables 2 and 3) indicate a moderate to intense weathering of first cycle sediment, or alternatively, recycling could have produced these rocks.

6. Conclusions

The Ordovician Khabour Formation in subsurface sections of west Iraq and in surface section of extreme north Iraq consists of sandstones and shales. Whereas, sandstone units of Devonian-Carboniferous Kaista Formation intercalate with limestone and shales The provenance of these formations has been assessed using integrated petrographical and geochemical data of the interbedded sandstones and shales to arrive at an internally consistent interpretation. The Khabour sandstones are subarkose and sublitharenite with few quartzarenite and derived largely from recycled orogen and continental block provenances while Kaista sandstones are mostly quartzarenite from recycled orogen. Both studied sandstones are predominantly derived from a felsic and rare mafic sources with a component from pre-existing sedimentary and volcanic rocks. Compositional differences and increase in the degree of weathering from sandstones to shales indicate climatic variations (semi-arid to humid) in the source area. In general, the acidic (felsic sources) and rare mafic sources with a prevailing continental margin tectonic setting for the Khabour sandstones, in accordance with higher values of Thorium/Scandium (Th/Sc) and Thorium/Uranium (Th/U) values seem that the felsic and mafic sources for the Khabour sandstone are likely consisted of basement rocks of Iraq. The Kaista sandstones were recycled from older sedimentary succession and were deposited in a fluvio-marine depositional system with dominating moderate to high degree of weathering in low plains regions and from semi-arid to semi-humid climate conditions.

7. References

Absar, N., Raza, M., Roy, M., Naqvi, S.M. & Roy, A.K. (2009). Composition and weathering conditions of Paleoproterozoic upper crust of Bundelkhand craton, Central India: Records from geochemistry of clastic sediments of 1.9 Ga Gwalior Group. *Precambrian Research*, Vol.168, No. 3-4, 313-329.

Al-Hadidy, A.H. (2007). Paleozoic stratigraphic lexicon and hydrocarbon habitat of Iraq. *GeoArabi*a, Vol. 12, No. 1, 63-130.

Al-Juboury, A.I. & Al-Hadidy, A.H. (2008). Facies and depositional environment of the Devonian-Carboniferous succession of Iraq .Geological Journal, Vol. 43, No. 2-3, 383-396.

Al-Juboury, A.I. & Al-Hadidy, A.H. (2009). Petrology and depositional evolution of the Paleozoic rocks of Iraq, Marine & Petroleum Geology, Vol. 26, No.2, 208-231.

Al-Omari, F.S. & Sadiq, A. (1977). Geology of Northern Iraq, Dar Al-Kutib press, Mosul University, Iraq, 198pp.

Al-Sharhan, A.S. & Nairn, A.E.M. (1997). Sedimentary Basins and Petroleum Geology of the Middle East. Elsevier, Amsterdam, 843pp.

Armstrong-Altrin, J.S. (2009). Provenance of sands from Cazones, Acapulco, and Bahía Kino beaches, México. *Revista Mexicana de Ciencias Geológicas*, Vol. 26, (3), 764-782

Armstrong-Altrin, J.S. & Verma, S.P. (2005). Critical evaluation of six tectonic setting discrimination diagrams using geochemical data of Neogene sediments from known tectonic settings. *Sedimentary Geology*, Vol. 177, 115-129.

Armstrong-Altrin, J.S., Lee, Y.I., Verma, S.P., Ramasamy, S. (2004). Geochemistry of sandstones from the upper Miocene Kudankulam Formation, Southern India: Implications for provenance, weathering, and tectonic setting. *Journal of Sedimentary Research,* Vol.74, No.2, 285-297.

Bakkiaraji, D., Nagendrai, R., Nagarajan, R. & Armstrong-Altrin, J.S. (2010). Geochemistry of sandstones from the Upper Cretaceous Sillakkudi Formation, Cauvery Basin, Southern India: Implication for Provenance. Journal of the Geological Society of India, Vol.76, 453-467.

Basu, A., Young, S., Suttner, L., James, W. & Mack, G.H. (1975). Re-evaluation of the use of undulatory extinction and crystallinity in detrital quartz for provenance interpretation. *Journal of Sedimentary Petrology*, Vol.45, 873-882.

Bauluz, B., Mayayo, M.J., Femandez-Nieto, C. & Gonzalez-Lopez, J.M. (2000). Geochemistry of Precambrian Paleozoic siliciclastic rocks from the Iberian Range (NE Spain): implication for source area weathering, sorting, provenance and tectonic setting. *Chemical Geology*, Vol.168, 135- 150.

Best, J.A., Barazangi, M., Al-Saad, D., Sawaf, T. & Gebran, A.. (1993). Continental margin evolution of the northern Arabian platform in Syria. *American Association of Petroleum Geologists Bulletin*, Vol.77 , No.2, 173-193.

Beydoun, Z.R. (1991). Arabian plate hydrocarbon, geology and potential: A plate tectonic approach, *AAPG Studies in Geology*, 33, 77pp.

Bhatia, M.R. (1983). Plate tectonics and geochemical composition of sandstones. *Geology*, Vol. 91, 611-627.

Bhatia, M.R. & Crook, K.A. W. (1986). Trace elements characteristics of greywackes and tectonic setting discrimination of sedimentary basins. *Contribution to Mineralogy and Petrology*, Vol.92, 181-193.

Bhushan, S.K. & Sahoo, P. (2010). Geochemistry of clastic sediments from Sargur supracrustals and Bababudan Group, Karnataka: implications on Archaean Proterozoic Boundary. *Journal Geological Society of India*, Vol.75, 829-840.

Buday, T. (1980). The Regional of Iraq. Vol.1, Stratigraphy & Palaeogeography. State Organization for Minerals, Baghdad, Iraq, 445pp.

Buday, T. & Jassim, S.Z. (1987). The Regional Geology of Iraq, vol. 2, Tectonism, Magmatism and Metamorphism. Publication of the Geological Survey of Iraq. Vol.2, 352p.

Cardenas, A., Girty, G.H., Hanson, A.D. & Lahren, M.M. (1996). Assessing differences in composition between low metamorphic grade mudstones and high-grade schists using log ratio techniques. *Journal of Geology*, Vol.104, 279-293.

Chakrabarti, G., Shome, D., Bauluz, B. & Sinha, S. (2009). Provenance and weathering history of Mesoproterozoic clastic sedimentary rocks from the Basal Gulcheru Formation, Cuddapah Basin, India. *Journal Geological Society of India,* Vol.74, 119-130.

Condie, K.C. (1991). Another look at rare earth elements in shales. *Geochimica et Cosmochimica Acta*, Vol.55, 2527-2531.

Cullers, R.L. (1994). The controls on the major and trace element variation of shales, siltstones and sandstones of Pennsylvanian-Permian age from uplifted continental blocks in Colorado to platform sediment in Kansas, USA. *Geochimica et Cosmochimica Acta*, Vol. 58, No.22, 4955-4972.

Cullers., R.L. (2002). Implications of elemental concentrations for provenance, redox conditions, and metamorphic studies of shales and limestones near Pueblo, CO, USA. *Chemical Geology*, Vol. 191, No.4, 305-327.

Cullers, R.L. & Podkovyrov, V.N. (2002). The source and origin of terrigenous sedimentary rocks in the Mesoproterozoic Ui group, southeastern Russia. *Precambrian Research* Vol.117, 157-183.

Cullers, R.L., Barret, T., Carlson, R. & Robinson, B. (1987). Rare earth element and mineralogical changes in Holocene soil and stream sediment: a case study in the Wet Mountains, Colorado, USA. *Chemical Geology*, Vol. 63, 275-295.

Das, B.K., AL-Mikhlafi, A.S. & Kaur, P. (2006). Geochemistry of Mansar Lake sediments, Jammu, India: Implication for source-area weathering, provenance, and tectonic setting. *Journal of Asian Earth Sciences*, Vol.26, 649-668.

De Araújo, C.E.G., Pinéo, T.R.G., Caby, R., Costa, F.G., Cavalcante, J.C., Vasconcelos, A.M. & Rodrigues, J.B. (2010). Provenance of the Novo Oriente Group, southwestern Ceará Central Domain, Borborema Province (NE-Brazil): A dismembered segment of a magma-poor passive margin or a restricted rift-related basin?. *Gondwana Research*, Vol.18, 497–510.

Dickinson, W.R. (1985). Interpreting detrital modes of greywacke and arkose. *Journal Sedimentary Petrology*, Vol.40, 695-707.

Dickinson, W.R. & Suczek, C.A. (1979). Plate tectonics and sandstone compositions. *American Association of Petroleum Geologist Bulletin*, Vol. 63, 2164-2182.

Dickinson, W.R., Beard, L. S., Brakenridge, G.R., Evjavec, J.L., Ferguson, R.C., Inman, K.F., Knepp, R.A., Lindberg, F.A. & Ryberg, P.T. (1983). Provenance of North American Phanerozoic sandstones in relation to tectonic setting. *Geological Society of America Bulletin*, Vol.94, 222-235.

Dokuz, A. & Tanyolu, E. (2006). Geochemical constraints on the provenance, mineral sorting and subaerial weathering of lower Jurassic and upper Cretaceous clastic rocks of the eastern Pontides, Yusufeli (Artvin), NE Turkey. *Turkish Journal of Earth Sciences,* Vol.15, 181-209.

Dostal, J. & Keppie, J.D. (2009). Geochemistry of low-grade clastic rocks in the Acatl n Complex of southern Mexico: Evidence for local provenance in felsic-intermediate igneous rocks. *Sedimentary Geology*, Vol.222, 241-253.

Drobe, M., Lpez de Luchi, M.G., Steenken, A., Frei, R., Naumann, R., Siegesmund, S. & Wemmera, K. (2009). Provenance of the late Proterozoic to early Cambrian metaclastic sediments of the Sierra de San Luis (Eastern Sierras Pampeanas) and Cordillera Oriental, Argentina. *Journal of South American Earth Sciences* , Vol.28, 239-262.

Etemad-Saeed, N., Hosseini-Barzi, M. & Armstrong-Altrin, J.S. (2011). Petrography and geochemistry of clastic sedimentary rocks as evidences for provenance of Lower Cambrian Lalun Formation, Posht-e-badam block, Central Iran, *Journal of African Earth Sciences*, Vol.61, No.2, 142-159.

Floyd, P.A. & Leveridge, B.E. (1987). Tectonic environment of the Devonian Gramscatho basin, south Cornwall: framework mode and geochemical evidence from turbiditic sandstones. *Journal of the Geological Society London* , Vol.144, 531-542.

Floyd, P.A., Winchester, J.A. & Park, R.G. (1989). Geochemistry and tectonic setting of Lewisianclastic metasediments from the Early Proterozoic Loch Maree Group of Gairloch, N.W. Scotland. *Precambrian Research* , Vol.45, No. 1-3, 203-214.

Folk, R.L. (1974). Petrology of Sedimentary Rocks, Hemphill Publication Company, Texas, 170pp.

Gabo, J.A.S., Dimalanta, C.B., Asio, M.G.S., Queao, K.L., Yumul Jr, G.P. & Imai, A. (2009). Geology and geochemistry of the clastic sequence from northwestern Panay (Philippines): Implications for provenance and geotectonic setting. *Tectonophysics*, Vol.479, 111-119.

Grantham, J.H. & Velbel, M.A. (1988). The influence of climate and topography on rock fragments abundance in modern fluvial sands of the southern Blue Ridge Mountains, North Carolina, *Journal of Sedimentary Petrology*, Vol.58, 219-227.

Hossain, H.M.Z., Roser, B.P. & Kimura, J.I. (2010). Petrography and whole-rock geochemistry of the Tertiary Sylhet succession, northeastern Bengal Basin, Bangladesh: provenance and source area weathering. *Sedimentary Geology*, Vol.228,171–183.

Husseini, M. I. (1992). Upper Paleozoic tectono-sedimentary evolution of the Arabian and adjoining plates. *Journal of the Geological Society*, London, Vol. 149, 419-429.

Ingersoll R. V. & Suczek C.A. (1979). Petrology and Provenance Neogene sand from Nicobar and Bengal fans. DSDP site 211and 218. *Journal of Sedimentary Petrology*. Vol.49. 1217-1228.

Jafarzadeh, M. & Hosseini-Barzi, M. (2008). Petrography and geochemistry of Ahwaz sandstone member of Asmari Formation, Zagros, Iran: implications on provenance and tectonic setting. *Revista Mexicana de Ciencias Geolgicas*, Vol.25, No.2, 247-260.

Karim, K.H. (2006). Comparison study between the Khabour and Tanjero Formations from North Iraq. Iraqi Journal of Earth Science, Mosul University,Vol. 6, No. 2, 1-12.

Kröner, A. & Sengör, A.M.C. (1990). Archean and Proterozoic ancestry in late Precambrian to early Paleozoic crustal elements of southern Turkey as revealed by single-zircon dating. *Geology*, Vol. 18 (12), 1186-1190.

Madhavaraju, J. & Lee, Y.I. (2010). Influence of Deccan volcanism in the sedimentary rocks of Late Maastrichtian–Danian age of Cauvery basin Southeastern India: constraints from geochemistry. *Current Science* , Vol.98, No.4, 528-537.

Maslov, A.V., Gareev, E.Z. & Podkovyrov, V.N. (2010). Upper Riphean and Vendian sandstones of the Bashkirian anticlinorium. *Lithology and Mineral Resources*, Vol. 45, No. 3, 285-301.

McGillivray, J.G. & Husseini, M.I. (1992). The Paleozoic petroleum geology of central Arabia. *American Association of Petroleum Geologists Bulletin*, Vol. 76, 1473-1490.

McLennan, S.M. (1989). Rare earth elements in sedimentary rocks: influence of provenance and sedimentary processes, in: Lipin, B.R., McKay G.A. (Eds.), Geochemistry and mineralogy of rare earth elements. *Reviews in Mineralogy*, Vol.21,169-200.

McLennan, S.M., & Taylor, S.R. (1991). Sedimentary rocks and crustal evolution, Tectonic setting and secular trend, *Journal of Geology*, Vol. 99, 1-21

McLennan, S.M., Taylor, S.R., McCulloch, M.T. & Maynard, J.B. (1990). Geochemical and Nd-Sr isotopic composition of deep-sea turbidites: Crustal evolution and plate tectonic associations. *Geochimica et Cosmochimica Acta*, Vol.54, 2015-2050.

McLennan, S.M., Hemming, S., McDaniel, D.K. & Hanson, G.N. (1993). Geochemical approaches to sedimentation, provenance and tectonics, in: Johnsson, M.J. and Basu, A. (Eds.), Processes Controlling the Composition of Clastic Sediments. *Geological Society of American Special Paper*, 21–40.

Murali, A.V., Parthasarathy, R., Mahadevan, T.M. & Sankar Das M. (1983). Trace element characteristics, REE patterns and partition coefficients of zircons from different geological environment- a case study on Indian zircons. Geochimica *et Cosmochimica Acta*, Vol.47, 2047-2052.

Nagarajan, R., Madhavaraju, J., Nagendra, R., Armstrong-Altrin, J.S. & Moutte, J. (2007). Geochemisrty of Neoproterozoic shales of the Rabanpalli Formation Bhima Basin, Northern Karnataka, southern India: implications for provenance and paleoredox conditions. *Revista Mexicana de Ciencias Geologicas* , Vol.24, 20-30.

Nesbitt, H.W. & Young, G.M. (1982). Early Proterozoic climates and plate motions inferred from major element chemistry of lutites. *Nature* , Vol.299, 715-717.

Nesbitt, H.W. & Young, G.M. (1996). Petrogenesis of sediments in the absence of chemical weathering: effects of abrasion and sorting on bulk composition and mineralogy. *Sedimentology*, Vol.43, 341-358.

Nesbitt, H.W., Fedo, C.M. & Young, G.M. (1997). Quartz and feldspar stability, steady and non steady state weathering and petrogenesis of siliciclastic sands and muds. *Journal of Geology*, Vol.105, 173-191.

Numan, N.M.S. (1997). A Plate tectonic scenario for the Phanerozoic succession in Iraq. *Iraqi Geological Journal,* Vol. 30, No. 2, 85-110.

Pettijohn, F.J. Potter, P.E. & Siever, R. (1987). Sand and Sandstones. Springer, New York, 553 pp.

Ranjan, N. & Banerjee, D.M. (2009). Central Himalayan crystalline as the primary source for the sandstone-mudstone suites of the Siwalik Group: New geochemical evidence. *Gondwana Research*, Vol.16, No. 3-4, 687-696.

Roser, B.P. & Korsch, R.J. (1986). Determination of tectonic setting of sandstone-mudstone suites using SiO2 content and K_2O/Na_2O ratio. *Journal of Geology*, Vol. 94, 635-650. Bhatia M.R. (1985). Plate tectonics and geochemical composition of sandstones: a reply. *Journal of Geology*, Vol. 93, 85-87.

Roser, B.P. & Korsch, R.J. (1988). Provenance signatures of sandstone-mudstone suite determined using discriminant function analysis of major-element data. *Chemical Geology,* Vol. 67,119-139.

Sharland, P.R., Archer, R., Casey, D.M., Davies, R.B., Hall, S.H., Heward, A.P., Horbury, A.D. & Simmons, M.D. (2001). Arabian Plate Sequence Stratigarphy, *GeoArabia Special Publicatio 2,* Gulf Petrolink, Bahrain, 371p

Sloss, L.L. (1963). Sequences in the cratonic interior of North America, Geological Society of America Bulletin, Vol.74, 93-114.

Suttner, L.J. & Dutta, P.K. (1986). Alluvial sandstone composition and paleoclimate, 1. Framework mineralogy. *Journal of Sedimentary Petrology*, Vol. 56, No.2, p. 329-345.

Suttner, L.J., Basu, A. & Mack, G.H. (1981). Climate and origin of quartzarenites. *Journal of Sedimentary Petrology*, Vol.51, 1235-1246.

Sun, S. S. & McDonough, W. F. (1989). Chemical and isotopic systematic of oceanic basalt: implication for mantle composition and processes. In: Saunders, A. D. & Norry, M. J., *Magmatism in the oceanic basins,* Spec. Publ. Geol. Soc. London. Vol. 42, 313-346.

Taylor, S.R. & McLennan, S. (1985). The Continental Crust, its Composition and Evolution, Blackwell, Oxford, 312p.

Taylor, S.R. & McLennan, S.M. (1995). The geochemical evolution of the continental crust. *Reviews in Geophysics*, Vol. 33: 241-265

Umazano, A.M., Bellosi, E.S., Visconti, G., Jalfin, A.G. & Melchor, R.N. (2009). Sedimentary record of a Late Cretaceous volcanic arc in central Patagonia: petrography, geochemistry and provenance of fluvial volcaniclastic deposits of the Bajo Barreal Formation, San Jorge Basin, Argentina. *Cretaceous Research* , Vol.30, 749-766.

van Bellen, R.C., Dunnington, H., Wetzel, R. & Morton, D.M. (1959). Lexique Stratigraphique International, Paris, centre National recherché Scientifique Fasc. 10a, Iraq, 333pp.

Weltje, G.J. (1994). Provenance and dispersal of sand-sized sediments: reconstruction of dispersal patterns and sources of sand-size sediments by means of inverse modeling techniques, PhD thesis, Geologicaa Ultraiectina.

Wani, H. & Mondal, M.E.A. (2010). Petrological and geochemical evidence of the Paleoproterozoic and the Meso-Neoproterozoic sedimentary rocks of the Bastar craton, Indian Peninsula: Implications on paleoweathering and Proterozoic crustal evolution. *Journal of Asian Earth Sciences*, Vol.38, 220-232.

Yerino, L.N. & Maynard, J.B. (1984). Petrography of 7 modern marine sands from the Peru-ChileTrench and adjacent areas. *Sedimentlogy*, Vol.31, 83-89.

Zimmermann, U. & Spalletti, L.A. (2009). Provenance of the Lower Paleozoic Balcarce Formation (Tandilia System, Buenos Aires Province, Argentina): Implications for paleogeographic reconstructions of SW Gondwana. *Sedimentary Geology*, Vol.219, 7-23.

Zuffa, G.G. (1987). Unravelling hinterland and offshore paleogeography of deep-water arenites. In, J.K. Leggett and G.G. Zuffa (Eds.). Marine Clastic Sedimentology, Concepts and Case Studies, London, Graham and Trotman, 39-61.

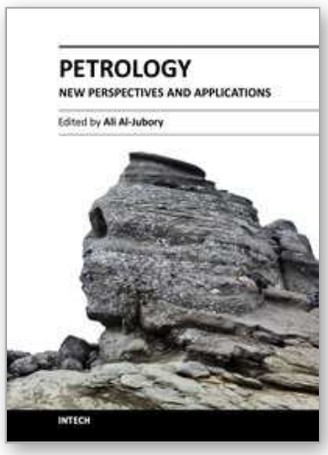

Petrology - New Perspectives and Applications

Edited by Prof. Ali Al-Juboury

ISBN 978-953-307-800-7
Hard cover, 224 pages
Publisher InTech
Published online 13, January, 2012
Published in print edition January, 2012

Petrology, New Perspectives and Applications is designed for advanced graduate courses and professionals in petrology. The book includes eight chapters that are focused on the recent advances and application of modern petrologic and geochemical methods for the understanding of igneous, metamorphic and even sedimentary rocks. Research studies contained in this volume provide an overview of application of modern petrologic techniques to rocks of diverse origins. They reflect a wide variety of settings (from South America to the Far East, and from Africa to Central Asia) as well as ages ranging from late Precambrian to late Cenozoic, with several on Mesozoic/Cenozoic volcanism.

InTech Europe
University Campus STeP Ri
Slavka Krautzeka 83/A
51000 Rijeka, Croatia
Phone: +385 (51) 770 447
Fax: +385 (51) 686 166
www.intechopen.com

InTech China
Unit 405, Office Block, Hotel Equatorial Shanghai
No.65, Yan An Road (West), Shanghai, 200040, China
中国上海市延安西路65号上海国际贵都大饭店办公楼405单元
Phone: +86-21-62489820
Fax: +86-21-62489821

IntechOpen